Molecular Biology of the Cell
Vol. 15, 3418–3432, July 2004

Cdc50p, a Protein Required for Polarized Growth, Associates with the Drs2p P-Type ATPase Implicated in Phospholipid Translocation in *Saccharomyces cerevisiae*

Koji Saito,* Konomi Fujimura-Kamada,* Nobumichi Furuta,* Utako Kato,† Masato Umeda,† and Kazuma Tanaka*‡

*Division of Molecular Interaction, Institute for Genetic Medicine, Hokkaido University Graduate School of Medicine, Sapporo 060-0815, Japan; and †Division of Molecular Biology and Information, Institute for Chemical Science, Kyoto University, Kyoto 611-0011, Japan

Submitted November 20, 2003; Revised April 5, 2004; Accepted April 8, 2004
Monitoring Editor: Randy Schekman

Cdc50p, a transmembrane protein localized to the late endosome, is required for polarized cell growth in yeast. Genetic studies suggest that *CDC50* performs a function similar to *DRS2*, which encodes a P-type ATPase of the aminophospholipid translocase (APT) subfamily. At low temperatures, *drs2*Δ mutant cells exhibited depolarization of cortical actin patches and mislocalization of polarity regulators, such as Bni1p and Gic1p, in a manner similar to the *cdc50*Δ mutant. Both Cdc50p and Drs2p were localized to the *trans*-Golgi network and late endosome. Cdc50p was coimmunoprecipitated with Drs2p from membrane protein extracts. In *cdc50*Δ mutant cells, Drs2p resided on the endoplasmic reticulum (ER), whereas Cdc50p was found on the ER membrane in *drs2*Δ cells, suggesting that the association on the ER membrane is required for transport of the Cdc50p-Drs2p complex to the *trans*-Golgi network. Lem3/Ros3p, a homolog of Cdc50p, was coimmunoprecipitated with another APT, Dnf1p; Lem3p was required for exit of Dnf1p out of the ER. Both Cdc50p-Drs2p and Lem3p-Dnf1p were confined to the plasma membrane upon blockade of endocytosis, suggesting that these proteins cycle between the exocytic and endocytic pathways, likely performing redundant functions. Thus, phospholipid asymmetry plays an important role in the establishment of cell polarity; the Cdc50p/Lem3p family likely constitute potential subunits specific to unique P-type ATPases of the APT subfamily.

INTRODUCTION

Cell polarity is the ultimate manifestation of the complex mechanisms that establish and maintain functionally specialized domains within the plasma membrane and cytoplasm. The asymmetric organization of the cytoskeleton, secretory pathway, and plasma membrane along an appropriate axis is established by specific proteins assembling a polarized and specialized cortical actin cytoskeleton (for review, see Drubin and Nelson, 1996). Polarized actin networks then mediate sorting and delivery of factors required to execute and maintain cell polarity.

The budding yeast *Saccharomyces cerevisiae* is an excellent model system to study the regulation of cell and cytoskeletal polarity (for reviews, see Pringle *et al*., 1995; Drubin and Nelson, 1996). During *S. cerevisiae* budding, the rigid cell wall is expanded locally as a result of polarized secretion. Cell surface extensions are preceded by the polarized organization of actin filament-containing structures, including actin cortical patches and actin cables. Cortical actin patches, small foci of actin filaments and associated proteins, cluster near regions of growth (for review, see Pruyne and Bretscher, 2000). These structures are required during endocytosis for internalization (for reviews, see Geli and Riezman, 1998; Wendland *et al*., 1998). Actin cables, bundles of actin filaments arising from discrete regions of the plasma membrane coincident with growth sites, extend throughout the cell. These dynamic cables guide the polarized movements of a type V myosin, Myo2p, to deliver secretory vesicles (Govindan *et al*., 1995; Schott *et al*., 1999).

Myo3p and Myo5p, *S. cerevisiae* type I myosins, are components of cortical patches aiding in the assembly of cortical actin patches. We isolated *CDC50* as a multicopy suppressor of the temperature-sensitive *myo3*Δ *myo5-360* mutant (Misu *et al*., 2003). The *cdc50*Δ mutant displays cold-sensitive cell cycle arrest with small buds. Arrested *cdc50*Δ cells are large and round, exhibiting depolarization of cortical actin patches and defects in the formation of actin cables. In addition, polarity regulators, Bni1p and Gic1p, are mislocalized in the *cdc50*Δ mutant cells. Bni1p, a component of the 12S polarisome, is a yeast counterpart of mammalian formin and is capable of polymerizing actin (Evangelista *et al*., 1997; Evangelista *et al*., 2002; Sagot *et al*., 2002). Gic1p is a downstream effector of the Cdc42p small GTPase, physically and functionally interacting with 12S polarisome components

Article published online ahead of print. Mol. Biol. Cell 10.1091/mbc.E03–11–0829. Article and publication date are available at www.molbiolcell.org/cgi/doi/10.1091/mbc.E03–11–0829.

‡ Corresponding author. E-mail address: k-tanaka@igm.hokudai.ac.jp.

Abbreviations used: APT, aminophospholipid translocase; CCV, clathrin-coated vesicle; DIC, differential interference contrast; ER, endoplasmic reticulum; GFP, green fluorescent protein; HA, hemagglutinin; mRFP1, monomeric red fluorescent protein 1; NBD, 7-nitrobens-2-oxa-1,3-diazol-4-yl; NBD-PE, 1-palmitoyl-2-(6-NBD-aminocaproyl)-PE; NBD-PC, 1-palmitoyl-2-(6-NBD-aminocaproyl)-PC; NBD-PS, 1-palmitoyl-2-(6-NBD-aminocaproyl)-PS; PCR, polymerase chain reaction; PE, phosphatidylethanolamine; PC, phosphatidylcholine; PS, phosphatidylserine; TGN, *trans*-Golgi network.

© 2004 by The American Society for Cell Biology

(Brown *et al*., 1997; Chen *et al*., 1997; Jaquenoud and Peter, 2000).

Cdc50p, a conserved integral membrane-spanning protein, is localized primarily to late endosomal/prevacuolar compartments, raising the question of how *CDC50* controls the localization of polarity regulators. Mutations of *LEM3/ROS3*, encoding a protein homologous to Cdc50p, confer hypersensitivity to a phosphatidylethanolamine-binding peptide antibiotic, Ro09-0198 (Kato *et al*., 2002). Interestingly, a mutant of *LEM3* also displays marked decreases in internalization of fluorescently 7-nitrobenz-2-oxa-1,3-diazol-4-yl (NBD)-labeled analogs of phosphatidylethanolamine (PE) and phosphatidylcholine (PC), but not of phosphatidylserine (PS) (Kato *et al*., 2002; Hanson *et al*., 2003). Lem3p is primarily localized to the plasma membrane, suggesting its involvement in the translocation of phospholipids across the plasma membrane.

The role of specific changes in phospholipid composition of intracellular or plasma membranes in the regulation of development or the maintenance of cell polarity remains unknown. Most cell types display an asymmetric distribution of phospholipids across the plasma membrane (Devaux, 1991; Cerbon and Calderon, 1991; Diaz and Schroit, 1996). In general, aminophospholipids PS and PE are enriched in the inner leaflet facing the cytoplasm, whereas PC, sphingomyelin, and glycolipids are predominantly found in the outer leaflet of the plasma membrane. In the human erythrocyte membrane, 80% of total PE and most of PS are found in the inner leaflet, whereas 76 and 82% of total PC and sphingomyelin are found in the outer leaflet, respectively (Rothman and Lenard, 1977). Similarly, in the budding yeast plasma membrane, 85 and 90% of total PE and PS are found in the inner leaflet, respectively (Cerbon and Calderon, 1991). Loss of this asymmetric distribution triggers a variety of intercellular events. Cell surface exposure of PS promotes platelet activation (Rosing *et al*., 1980) and acts as a signal for the recognition and removal of apoptotic cells by macrophages (Fadok *et al*., 2000). Lipid asymmetry is generated and maintained by ATP-driven lipid transporters or translocases (Devaux, 1991), a prime candidate aminophospholipid translocase (APT) of which is ATPase II (Zachowski *et al*., 1989). Molecular cloning of the ATPase II-encoding gene from bovine chromaffin granules revealed it as a member of a previously unrecognized subfamily of P-type ATPases (Tang *et al*., 1996). Members of this subfamily differ from cation-transporting P-type ATPases because they lack the negatively charged amino acids within the transmembrane segments critical for cation transport.

Of the five members of this subfamily in *S. cerevisiae*, *DRS2*, *NEO1*, *DNF1*, *DNF2*, and *DNF3* (Hua *et al*., 2002), the functions of Drs2p are the best characterized. *DRS2* was identified as a mutation that is synthetically lethal with a mutation in *ARF1*, which encodes an ADP-ribosylation factor (*ARF*) (Chen *et al*., 1999). *ARF* is a small GTPase involved in initiating the formation of COPI and clathrin-coated vesicles (CCVs). Drs2p is localized to the *trans*-Golgi network (TGN). The *drs2*Δ mutant exhibits TGN defects comparable with those exhibited by strains with clathrin mutations (Chen *et al*., 1999). The *drs2*Δ mutant also exhibits a defect in APT activity at the plasma membrane (Tang *et al*., 1996), although this result remains in dispute (Siegmund *et al*., 1998; Marx *et al*., 1999). The lack of detectable differences in APT activity in *drs2*Δ mutant cells may be due to Drs2p localization to the TGN. In contrast, loss of Dnf1p and Dnf2p abolishes the ATP-dependent transport of NBD-labeled PE, PC, and PS across the plasma membrane (Pomorski *et al*., 2003). Because Dnf1p and Dnf2p are localized to the plasma membrane, these proteins are likely the P-type ATPases responsible for the translocation of phospholipids at the plasma membrane.

Because Lem3p and Cdc50p are not structurally related to ATPases, it remains unclear whether Lem3p possesses an APT activity, or functions in conjunction with a P-type ATPase or another APT. Here, we show that the *cdc50*Δ and *drs2*Δ mutants show similar phenotypes, including cold-sensitive growth, depolarization of cortical actin patches and mislocalization of polarity regulators. Although the *lem3*Δ or *dnf1*Δ mutation does not affect cell growth, they show synthetic lethal interaction with *cdc50*Δ and *drs2*Δ mutations. Coimmunoprecipitation experiments also demonstrate that Cdc50p and Lem3p associate with Drs2p and Dnf1p, respectively. Cdc50p and Lem3p also are required for proper localization of Drs2p and Dnf1p, respectively. We therefore propose that the Cdc50p/Lem3p family comprises a set of subunits specific to phospholipid-translocating P-type ATPases.

MATERIALS AND METHODS

Media and Genetic Techniques

Unless otherwise specified, strains were grown in YPDA rich medium (1% yeast extract [Difco, Detroit, MI], 2% bacto-peptone [Difco], 2% glucose, and 0.01% adenine). Strains carrying plasmids were selected in synthetic medium (SD) containing the required nutritional supplements (Rose *et al*., 1990). When indicated, 0.5% casamino acids (Difco) were added to SD medium without uracil (SDA-Ura). Standard genetic manipulations of yeast were performed as described previously (Guthrie and Fink, 1991). Yeast transformations were performed using the lithium acetate method (Elble, 1992; Agatep *et al*., 1998). *Escherichia coli* strains DH5α and XL1-Blue were used for construction and amplification of plasmids.

Strains and Plasmids

Yeast strains used in this study are summarized in Table 1. Yeast strains carrying complete gene deletions (*LEM3*), 3 × hemagglutinin (HA)-tagged genes (*CDC50*, *LEM3*), 13 × Myc-tagged genes (*DRS2*, *DNF1*, and *NEO1*), enhanced green fluorescent protein (EGFP)-tagged genes (*DRS2*, *DNF1*, *NEO1*, *CDC50*, and *SEC7*), and the monomeric red fluorescent protein 1 (mRFP1)-tagged *SEC7* gene were constructed by polymerase chain reaction (PCR)-based procedures as described previously (Longtine *et al*., 1998). The *vrp1* and *vp527* disruption mutants were constructed as described by Mochida *et al*. (2002) and by Misu *et al*. (2003), respectively. The *drs2* and *dnf1* disruption mutants were constructed on our strain background as follows. Regions containing the disruption marker and the flanking sequences were PCR amplified using genomic DNA derived from either the *drs2*Δ*::KanMX4* or *dnf1*Δ*::KanMX4* strains (a gift from C. Boone, University of Toronto, Ontario, Canada) as a template. The amplified DNA fragment was then introduced into the appropriate strain. All constructs produced by the PCR-based procedure were verified by colony-PCR amplification to confirm the replacement occurred at the expected locus. Epitope-tagged Drs2 and Neo1 proteins were deemed functional, because they supported cell growth at all temperatures tested. Epitope-tagged Dnf1 protein was also functional as *cdc50*Δ strain with the epitope-tagged Dnf1 protein was viable at permissive temperatures for *cdc50*Δ strain, whereas the *cdc50*Δ *dnf1*Δ strain was inviable at all temperatures (see below; Table 3). The *drs2*Δ*::hphMX4* and *dnf1*Δ*::hphMX4* strains were constructed by replacing the *KanMX4* cassette of YKT745 (*drs2*Δ*::KanMX4*) and YKT748 (*dnf1*Δ*::KanMX4*), respectively, with the *hphMX4* cassette from pAG32 (Goldstein and McCusker, 1999). The *drs2*Δ strain expressing *BNI1-EGFP* and *drs2*Δ strain expressing *GIC1-EGFP* were constructed by crosses of YKT745 (*drs2*Δ*::KanMX4*) with YKT455 (*BNI1-EGFP::KanMX6)* and YKT579 (*GIC1-EGFP::KanMX6*), respectively, followed by tetrad dissection. The *drs2*Δ strain expressing either *BNI1-EGFP* or *GIC1-EGFP* was confirmed by colony-PCR amplification.

The plasmid used to construct the *SEC7-mRFP1::TRP1* strain was created by PCR amplification of the mRFP1 gene by using the oligonucleotide primers PAmRFP1 (5′-GATTTAATTA ACATGGCCTC CTCCGAGGAC-3′) and mRFP1AS (5′-CTTGGCGCGC CTAGGCGCCG GTGGAGTG-3′) with the mRFP1 gene within the pRSET$_B$ plasmid (Campbell *et al*., 2002) as a template. The amplified fragment, followed by digestion with *Asc*I and *Pac*I, was cloned into the *Asc*I-*Pac*I gap of pFA6a-GFP-TRP1 (Longtine *et al*., 1998) to obtain a plasmid, designated pFA6a-mRFP1-TRP1, in which the original GFP is replaced with mRFP1. pRS416 *GFP-SNC1* was generously provided by M. Lewis and H. Pelham (Medical Research Council) (Lewis *et al*., 2000). The plasmids used in this study are summarized in Table 2. Schemes detailing the construction of plasmids are available upon request.

Table 1. *S. cerevisiae* strains used in this study

Strain[a]	Genotype	Reference or source
YEF473	*MAT***a**/α *lys2-801/lys2-801 ura3-52/ura3-52 his3Δ-200/his3Δ-200 trp1Δ-63/trp1Δ-63 leu2Δ-1/leu2Δ-1*	Longtine *et al.* (1998)
YKT38	*MAT***a** *lys2-801 ura3-52 his3Δ-200 trp1Δ-63 leu2Δ-1*	Misu *et al.* (2003)
YKT39	*MAT*α *lys2-801 ura3-52 his3Δ-200 trp1Δ-63 leu2Δ-1*	This study
YKT130	*MAT***a** *lys2-801 ura3-52 his3Δ-200 trp1Δ-63 leu2Δ-1 vrp1Δ::LEU2*	Mochida *et al.* (2001)
YKT249	*MAT***a** *lys2-801 ura3-52 his3Δ-200 trp1Δ-63 leu2Δ-1 cdc50Δ::HIS3MX6*	Misu *et al.* (2003)
YKT259	*MAT***a** *lys2-801 ura3-52 his3Δ-200 trp1Δ-63 leu2Δ-1 CDC50-EGFP::KanMX6*	This study
YKT283	*MAT*α *lys2-801 ura3-52 his3Δ-200 trp1Δ-63 leu2Δ-1 CDC50-3HA::HIS3MX6*	This study
YKT442	*MAT***a**/α *lys2-801/lys2-801 ura3-52/ura3-52 his3Δ-200/his3Δ-200 trp1 Δ-63/trp1Δ-63 leu2Δ-1/leu2Δ-1 cdc50Δ::HIS3MX6/cdc50Δ::HIS3MX6*	Misu *et al.* (2003)
YKT455	*MAT***a** *lys2-801 ura3-52 his3Δ-200 trp1Δ-63 leu2Δ-1 BNI1-EGFP::KanMX6*	Misu *et al.* (2003)
YKT495	*MAT***a** *lys2-801 ura3-52 his3Δ-200 trp1Δ-63 leu2Δ-1 cdc50Δ::HIS3MX6 BNI1-EGFP::KanMX6*	Misu *et al.* (2003)
YKT496	*MAT*α *lys2-801 ura3-52 his3Δ-200 trp1Δ-63 leu2Δ-1 lem3Δ::TRP1*	This study
YKT579	*MAT***a** *lys2-801 ura3-52 his3Δ-200 trp1Δ-63 leu2Δ-1 GIC1-EGFP::KanMX6*	Misu *et al.* (2003)
YKT580	*MAT***a** *lys2-801 ura3-52 his3Δ-200 trp1Δ-63 leu2Δ-1 cdc50Δ::HIS3MX6 GIC1-EGFP::KanMX6*	Misu *et al.* (2003)
YKT715	*MAT***a** *lys2-801 ura3-52 his3Δ-200 trp1Δ-63 leu2Δ-1 lem3Δ::TRP1*	This study
YKT745	*MAT*α *lys2-801 ura3-52 his3Δ-200 trp1Δ-63 leu2Δ-1 drs2Δ::KanMX4*	This study
YKT747	*MAT*α *lys2-801 ura3-52 his3Δ-200 trp1Δ-63 leu2Δ-1 drs2Δ::hphMX4*	This study
YKT748	*MAT***a** *lys2-801 ura3-52 his3Δ-200 trp1Δ-63 leu2Δ-1 dnf1Δ::KanMX4*	This study
YKT751	*MAT*α *lys2-801 ura3-52 his3Δ-200 trp1Δ-63 leu2Δ-1 cdc50Δ::HIS3MX6 drs2Δ::KanMX4*	This study
YKT754	*MAT*α *lys2-801 ura3-52 his3Δ-200 trp1Δ-63 leu2Δ-1 dnf1Δ::KanMX4 lem3Δ::TRP1*	This study
YKT755	*MAT*α *lys2-801 ura3-52 his3Δ-200 trp1Δ-63 leu2Δ-1 CDC50-3HA::HIS3MX6 DRS2-13Myc::TRP1*	This study
YKT759	*MAT*α *lys2-801 ura3-52 his3Δ-200 trp1Δ-63 leu2Δ-1 CDC50-3HA::HIS3MX6 DNF1-13Myc::TRP1*	This study
YKT761	*MAT*α *lys2-801 ura3-52 his3Δ-200 trp1Δ-63 leu2Δ-1 CDC50-3HA::HIS3MX6 NEO1-13Myc::TRP1*	This study
YKT768	*MAT*α *lys2-801 ura3-52 his3Δ-200 trp1Δ-63 leu2Δ-1 DRS2-EGFP::KanMX6*	This study
YKT769	*MAT***a** *lys2-801 ura3-52 his3Δ-200 trp1Δ-63 leu2Δ-1 cdc50Δ::HIS3MX6 DRS2-EGFP::KanMX6*	This study
YKT770	*MAT*α *lys2-801 ura3-52 his3Δ-200 trp1Δ-63 leu2Δ-1 lem3Δ::TRP1 DRS2-EGFP::KanMX6*	This study
YKT771	*MAT*α *lys2-801 ura3-52 his3Δ-200 trp1Δ-63 leu2Δ-1 DNF1-EGFP::KanMX6*	This study
YKT772	*MAT***a** *lys2-801 ura3-52 his3Δ-200 trp1Δ-63 leu2Δ-1 cdc50Δ::HIS3MX6 DNF1-EGFP::KanMX6*	This study
YKT773	*MAT*α *lys2-801 ura3-52 his3Δ-200 trp1Δ-63 leu2Δ-1 lem3Δ::TRP1 DNF1-EGFP::KanMX6*	This study
YKT774	*MAT*α *lys2-801 ura3-52 his3Δ-200 trp1Δ-63 leu2Δ-1 drs2Δ::hphMX4 CDC50-EGFP::KanMX6*	This study
YKT775	*MAT*α *lys2-801 ura3-52 his3Δ-200 trp1Δ-63 leu2Δ-1 NEO1-EGFP::KanMX6*	This study
YKT776	*MAT***a** *lys2-801 ura3-52 his3Δ-200 trp1Δ-63 leu2Δ-1 cdc50Δ::HIS3MX6 NEO1-EGFP::KanMX6*	This study
YKT777	*MAT***a** *lys2-801 ura3-52 his3Δ-200 trp1Δ-63 leu2Δ-1 vrp1Δ::LEU2 DRS2-EGFP::KanMX6*	This study
YKT779	*MAT*α *lys2-801 ura3-52 his3Δ-200 trp1Δ-63 leu2Δ-1 drs2Δ::KanM4 BNI1-EGFP::KanMX6*	This study
YKT781	*MAT*α *lys2-801 ura3-52 his3Δ-200 trp1Δ-63 leu2Δ-1 drs2Δ::KanMX4 GIC1-EGFP::KanMX6*	This study
YKT782	*MAT***a** *lys2-801 ura3-52 his3Δ-200 trp1Δ-63 leu2Δ-1 LEM3-3HA::TRP1*	This study
YKT788	*MAT***a**/α *lys2-801/lys2-801 ura3-52/ura3-52 his3Δ-200/his3Δ-200 trp1Δ-63/trp1Δ-63 leu2Δ-1/leu2Δ-1 SEC7-mRFP::TRP1/SEC7 CDC50-EGFP::KanMX6/CDC50*	This study
YKT789	*MAT***a**/α *lys2-801/lys2-801 ura3-52/ura3-52 his3Δ-200/his3Δ-200 trp1Δ-63/trp1Δ-63 leu2Δ-1/leu2Δ-1 SEC7-mRFP1::TRP1/SEC7 DRS2-EGFP::KanMX6/DRS2*	This study
YKT804	*MAT*α *lys2-801 ura3-52 his3Δ-200 trp1Δ-63 leu2Δ-1 vrp1Δ::LEU2 DNF1-EGFP::KanMX6*	This study
YKT805	*MAT*α *lys2-801 ura3-52 his3Δ-200 trp1Δ-63 leu2Δ-1 lem3Δ::TRP1 vrp1Δ::LEU2 CDC50-EGFP::KanMX6*	This study
YKT806	*MAT*α *lys2-801 ura3-52 his3Δ-200 trp1Δ-63 leu2Δ-1 lem3Δ::TRP1 vrp1Δ::LEU2 DRS2-EGFP:: KanMX6*	This study
YKT807	*MAT*α *lys2-801 ura3-52 his3Δ-200 trp1Δ-63 leu2Δ-1 LEM3-3HA::HIS3MX6 DNF1-13Myc::TRP1*	This study
YKT808	*MAT*α *lys2-801 ura3-52 his3Δ-200 trp1Δ-63 leu2Δ-1 LEM3-3HA::HIS3MX6*	This study
YKT809	*MAT***a** *lys2-801 ura3-52 his3Δ-200 trp1Δ-63 leu2Δ-1 LEM3-3HA::TRP1 DNF1-EGFP::KanMX6*	This study
YKT834	*MAT***a** *lys2-801 ura3-52 his3Δ-200 trp1Δ-63 leu2Δ-1 vrp1Δ::LEU2 CDC50-EGFP::KanMX6*	This study
YKT836	*MAT***a** *lys2-801 ura3-52 his3Δ-200 trp1Δ-63 leu2Δ-1 lem3Δ::TRP1 CDC50-EGFP::KanMX6*	This study
YKT839	*MAT*α *lys2-801 ura3-52 his3Δ-200 trp1Δ-63 leu2Δ-1 lem3Δ::TRP1 vrp1Δ::LEU2*	This study
YKT840	*MAT*α *lys2-801 ura3-52 his3Δ-200 trp1Δ-63 leu2Δ-1 vps27Δ::HIS3 DRS2-EGFP::KanMX6*	This study
YKT843	*MAT*α *lys2-801 ura3-52 his3Δ-200 trp1Δ-63 leu2Δ-1 lem3Δ::TRP1 vrp1Δ::KanMX6*	This study
YKT844	*MAT***a** *lys2-801 ura3-52 his3Δ-200 trp1Δ-63 leu2Δ-1 dnf1Δ::hphMX4*	This study
YKT913[b]	*MAT*α *ura3 his3 his4 trp1 leu2 suc2? gal2? sec12-4 CDC50-3HA::HIS3MX6 DRS2-13Myc::TRP1*	This study
YKT914[b]	*MAT***a** *ura3 his3 trp1 leu2 suc2? gal2? sec12-4 CDC50-3HA::HIS3MX6 DNF1-13Myc::TRP1*	This study
YKT915[b]	*MAT*α *lys2 ura3 his3 his4 trp1 leu2 suc2? gal2? sec12-4 CDC50-3HA::HIS3MX6*	This study
MBY10-7A	*MAT***a** *ura3 his3 his4 leu2 trp1 suc2 gal2 sec12-4*	A gift from A. Nakano

[a] YKT strains except for YKT913, 914, and 915 are isogenic derivatives of YEF473.

[b] YKT913 and YKT915 are segregant from a cross of MBY10-7A with YKT755. YKT914 is a segregant from a cross of MBY10-7A with YKT759.

Isolation of Multicopy Suppressors of the cdc50Δ Mutant

The *cdc50*Δ strain (YKT442) was transformed with a yeast genomic DNA library constructed in the YEp24 multicopy plasmid. As spontaneous revertants often arise in the *cdc50*Δ strain at the restrictive temperature (18°C), a homozygous diploid strain was used for the multicopy suppressor screening. After transformation, cells were first incubated at 30°C for 24 h to allow recovery, and then incubated at 18°C for 6 d on SDA-Ura plates. Approximately 570,000 transformants were screened; 41 transformants reproducibly grew at 18°C. The transformants containing *CDC50* on the plasmid were identified by colony PCR and eliminated. Plasmids were obtained from each of the remaining transformants for further analysis. All of them conferred cold temperature-resistant growth to YKT442. Plasmids

Table 2. Plasmids used in this study

Plasmid	Characteristics	Reference or source
pKT1266 [YEplac181 CDC50-EGFP]	*CDC50-EGFP LEU2 2μm*	Misu *et al.* (2003)
pKT1468 [YEplac195 DRS2]	*DRS2 URA3 2μm*	This study
pKT1472 [YEplac195 DRS2 CDC50]	*CDC50 DRS2 URA3 2μm*	This study
pRS416 GFP-SNC1	*GFP-SNC1 URA3 CEN*	Lewis *et al.* (2000)
YEplac181	*LEU2 2μm*	Gietz and Sugino (1988)
YEplac195	*URA3 2μm*	Gietz and Sugino (1988)

carrying the *LEM3* gene were identified by PCR and eliminated. The genes contained within the remaining seven plasmids were identified by sequencing both ends of the inserts, and then classified into three nonoverlapping groups. The group providing the strongest suppressor activity was analyzed. Deletion analysis revealed this suppressor gene as *NEO1*.

Antibodies

Mouse anti-HA (HA.11) and anti-Myc (9E10) monoclonal antibodies were purchased from Babco (Richmond, CA) and Sigma-Aldrich (St. Louis, MO), respectively. Rabbit anti-Lem3p polyclonal antibodies have been described previously (Kato *et al*., 2002). The horseradish peroxidase (HRP)-conjugated secondary antibodies (sheep anti-mouse IgG and donkey anti-rabbit IgG) used for immunoblotting were purchased from Amersham Biosciences (Piscataway, NJ). Cy3-conjugated secondary antibodies (donkey anti-mouse IgG) used for immunofluorescence were purchased from Jackson ImmunoResearch Laboratories (West Grove, PA).

Immunoprecipitation and Western Blotting

The preparation of crude membrane and soluble fractions was performed as described previously (Chang and Slayman, 1991) with the following modifications. Cells were grown at 25°C for 12 h to a cell density of 0.5 OD_{600}/ml in YPDA medium. Cells collected from 400 ml of cultures were washed three times in lysis buffer (10 mM Tris-HCl, pH 7.5, 0.3 M sorbitol, 0.1 M NaCl, 5 mM $MgCl_2$) and resuspended at 200 OD_{600}/ml in lysis buffer containing protease inhibitors (1 μg/ml aprotinin, 1 μg/ml leupeptin, 1 μg/ml pepstatin, 2 mM benzamidine, 1 mM phenylmetylsulfonylfluoride). The cells were then lysed by agitation six times with glass beads on a Vortex mixer for 30 s. Cell lysates were centrifuged at 400 × *g* for 5 min to remove unbroken cells; the supernatant was then centrifuged at 100,000 × *g* for 1 h at 4°C (TLA120.2 rotor; Beckman Coulter, Fullerton, CA). The supernatant was removed to obtain a pellet of total membranes. For immunoprecipitation, membrane pellets were solubilized in 0.8 ml of immunoprecipitation buffer (10 mM Tris-HCl, pH 7.5, 150 mM NaCl, 2 mM EDTA, 1% CHAPS) containing the above-mentioned protease inhibitors. Insoluble material was removed by centrifugation at 20,630 × *g* for 5 min at 4°C. The cleared lysates were split into two aliquots; each was incubated with 5 μg of either anti-Myc antibody or control mouse IgG for 1 h at 4°C. We then rotated these samples with 20 μl of protein G-Sepharose 4 Fast Flow (Amersham Biosciences AB, Uppsala, Sweden) for 1 h at 4°C. The protein G-Sepharose beads were then pelleted and washed three times with immunoprecipitation buffer in the absence of detergents. The immunoprecipitates were separated by SDS-PAGE and transferred to polyvinylidene difluoride membrane. Membranes were blocked in 5% skim milk in 50 mM Tris-HCl, pH 7.5, 200 mM NaCl with 0.05% Tween 20 (TBST) for 30 min at room temperature. Membranes were then incubated with primary antibody (anti-Myc antibody diluted 1:1000, anti-HA antibody diluted 1:1000, or anti-Lem3p antibodies diluted 1:1000 in 5% skim milk in TBST) at 4°C overnight. After three washes with 5% skim milk in TBST, the membrane was incubated in secondary antibody (anti-mouse IgG-HRP or anti-rabbit IgG-HRP diluted 1:1000 in TBST) for 1 h at room temperature. After three washes in TBST, membranes were visualized by chemiluminescence (Amersham Biosciences). Protein bands were detected using LAS1000plus (Fuji Film, Tokyo, Japan), and the signal intensity of the bands was quantified by Science Lab 2001 Image Gauge, version 4.0 (Fuji Film).

Lipid Preparation

1-Palmitoyl-2-(6-NBD-aminocaproyl)-PE (NBD-PE), 1-palmitoyl-2-(6-NBD-aminocaproyl)-PC (NBD-PC), 1-palmitoyl-2-(6-NBD-aminocaproyl)-PS (NBD-PS), and dioleoylphosphatidylcholine (DOPC) were obtained from Avanti Polar Lipids (Alabaster, AL). To prepare large unilamellar vesicles, lipids were mixed at 40 mol % NBD-PE, -PC, or -PS, and 60 mol % DOPC. Chloroform was removed by evaporation followed by vacuum desiccation. Desiccated phospholipids were solubilized in SD medium; the mixture was passed seven times through a LiposoFast-Basic stabilizer (Avanti, Ottawa, Canada), equipped with 0.1-μm filters to produce evenly sized vesicles containing a 1 mM total concentration of lipids.

Internalization of Fluorescence-labeled Phospholipids into Yeast Cells

Fluorescently labeled phospholipids internalization experiments were performed as described by Kato *et al.* (2002). Briefly, cells carrying the designated plasmids were grown to early-mid logarithmic phase in SD-Ura media at 25°C. After dilution to 0.35 OD_{600}/ml in SD-Ura, cells were incubated with vesicles containing 40% NBD-phospholipids and 60% DOPC at a final concentration of 50 μM, shaking for 30 min at 25°C. Cells were then suspended in SD medium containing 0.01% NaN_3 and 2.5 μg/ml propidium iodide (PI) to allow the exclusion of PI-positive dead cells in flow cytometric analysis. Flow cytometry of NBD-labeled cells was performed on a FACS Calibur cytometer by using CellQuest software (BD Biosciences, San Jose, CA). Green fluorescence of the NBD was plotted on a histogram to allow calculation of the mean fluorescence intensity.

Microscopic Observations

Cells were observed using a Nikon ECRIPSE E800 microscope (Nikon Instec, Tokyo, Japan) equipped with a HB-10103AF super high-pressure mercury lamp and a 1.4 numerical aperture 100× Plan Apo oil immersion objective (Nikon Instec) with the appropriate fluorescence filter sets (Nikon Instec) and differential interference contrast (DIC) optics. Images were acquired with a digital cooled charge-couple device camera (C4742–95-12NR; Hamamatsu Photonics, Hamamatsu, Japan) by using AQUACOSMOS software (Hamamatsu Photonics). Observations are compiled from the examination of at least 100 cells.

To visualize GFP-tagged proteins in living cells, cells were grown to early-mid logarithmic phase, harvested, and resuspended in SD medium. Cells were mounted on microslide glass and observed immediately using a GFP (green) bandpass filter set. To observe Bni1p-GFP and Gic1p-GFP, cells were fixed for 10 min at 18°C by direct addition of 37% formaldehyde (Wako Pure Chemicals, Osaka, Japan) to a final concentration of 2% as described previously (Kawasaki *et al*., 2003). Images of GFP-fusion proteins in fixed cells were similar to those observed in living cells.

To observe filamentous actin, cells were grown to early logarithmic phase, fixed in formaldehyde, and stained with tetramethylrhodamine isothiocyanate-phalloidin (Sigma-Aldrich) as described previously (Mochida *et al*., 2002). After six washes in phosphate-buffered saline, cells were mounted in 90% glycerol containing *n*-propyl gallate (Wako Pure Chemicals). Cells were immediately observed microscopically using a G-2A (red) bandpass filter set.

Lypophilic styryl dye *N*-(3-triethylammoniumpropyl)-4-(*p*-diethylaminophenylhexatrienyl) pyridinium dibromide (FM4-64) (Molecular Probes, Eugene, OR) staining was performed as described previously (Misu *et al*., 2003). Cells were grown to late logarithmic phase in YPDA medium at 30°C. Four OD_{600} units of cells were incubated with 32 μM FM4-64 at 30°C for 15 min in 100 μl of YPDA medium. Cells were harvested by centrifugation, resuspended in 200 μl of fresh YPDA medium, and chased at 30°C for 30 min. After the chase period, cells were washed twice in SD medium and immediately observed microscopically using a G-2A bandpass filter set.

The preparation of cells for Lem3p-HA immunofluorescence analysis was performed as described previously (Berkower *et al*., 1994). Cells were grown to mid-logarithmic phase in YPDA medium at 30°C. Cells were fixed in 4% formaldehyde at 30°C for 20 min, permeabilized, and incubated with a mouse anti-HA monoclonal antibody (HA.11) diluted at 1:2000. Antibody binding was visualized by treatment with Cy3-conjugated anti-mouse IgG antibodies diluted at 1:500 (Jackson ImmunoResearch Laboratories). After four washes in PBS, cells were mounted in 90% glycerol containing *n*-propyl gallate (Wako Pure Chemicals). Cells were observed microscopically using a G-2A bandpass filter set.

RESULTS

Isolation of NEO1 as a Multicopy Suppressor of the cdc50Δ Mutation

To identify genes involved in the regulation or function of Cdc50p, we isolated multicopy suppressors of the cold-

sensitive growth phenotype of *cdc50*Δ mutant at 18°C, and found *NEO1* in those genes. Overexpression of *NEO1* also suppressed the defects in actin cytoskeletal organization in the *cdc50*Δ mutant at 18°C. It increased both cell populations with polarized cortical actin patches and actin cables from <5% to ~30% of small-budded *cdc50*Δ mutant cells (our unpublished data). *NEO1* was originally isolated as a gene conferring resistance to the aminoglycoside neomycin upon overexpression (Prezant *et al*., 1996). The *NEO1* gene, a member of the yeast *DRS2/NEO1* family, encodes a P-type ATPase belonging to the APT subfamily (Catty *et al*., 1997). Other members of this family, Dnf1p, Dnf2p, and Drs2p, regulate transbilayer phospholipid arrangement (Pomorski *et al*., 2003). Overexpression of *DNF1* also partially suppressed a cold-sensitive growth defect of the *cdc50*Δ mutant at 18°C (our unpublished data).

In yeast, Cdc50p has two structural homologues, Lem3p/Ros3p and Ynr048wp. Here, we designate the *YNR048w* gene *CRF1* (CDC50/ROS3 family 1). A triple null mutant of *CDC50*, *LEM3*, and *CRF1* is not viable. Overexpression of either *LEM3* or *CRF1* suppresses the cold-sensitive growth defect of the *cdc50-1* mutant (Radji *et al*., 2001), demonstrating that these three genes constitute an essential gene family with substantial functional overlaps. We also isolated *LEM3* as a multicopy suppressor of the cold-sensitive growth defect of the *cdc50*Δ mutant at 18°C (see MATERIALS AND METHODS). Recent observations that the *lem3*Δ mutant displays defects in the internalization of fluorescently labeled phospholipids (Kato *et al*., 2002; Hanson *et al*., 2003) suggest that Cdc50p and Crf1p have similar biochemical functions. The *CDC50/LEM3* family may be functionally related to *DRS2/NEO1* family, although these two families are structurally unrelated. We therefore investigated the functional relationship between the *CDC50/LEM3* and *DRS2/NEO1* families.

Genetic Interaction between CDC50/LEM3 Family and DRS2/NEO1 Family

We examined the growth profile of cells lacking two of the *CDC50/LEM3* family members; the *cdc50*Δ *lem3*Δ mutant exhibited a severe growth defect, whereas the *cdc50*Δ *crf1*Δ mutant exhibited a similar cold-sensitive growth defect as seen in the *cdc50*Δ mutant. The *lem3*Δ *crf1*Δ mutant grew as well as wild-type cells (our unpublished data). These results indicate that *CDC50* and *LEM3* have substantial functional overlap in cell growth regulation, whereas *CRF1* contributes little in the absence of *CDC50* or *LEM3*. The investigation of Hua *et al.* (2002) into the genetic interactions among the members of the *DRS2/NEO1* family (*NEO1*, *DRS2*, *DNF1*, *DNF2*, and *DNF3*) revealed that *NEO1* is an essential gene with unique functions. The *drs2*Δ mutant exhibits a cold-sensitive growth phenotype, whereas *dnf1*Δ, *dnf2*Δ, or *dnf3*Δ single mutants grow normally at all temperatures tested. A *dnf1*Δ *dnf2*Δ *dnf3*Δ triple mutant also grows normally, at similar rate as seen for wild-type cells. The *drs2*Δ *dnf1*Δ mutant, however, displays a severe growth defect, whereas neither *dnf2*Δ nor *dnf3*Δ mutations exacerbated the growth phenotype of the *drs2*Δ mutant. These results indicate that *DRS2* and *DNF1* likely overlap in their functions during cell growth, whereas *DNF2* and *DNF3* contribute little to cell growth in the absence of *DRS2*.

We therefore investigated the genetic interactions between the *CDC50/LEM3* and *DRS2/DNF1* genes, which are the members of the *CDC50/LEM3* and *DRS2/NEO1* families that contribute most substantially to cell growth. We generated strains carrying combinations of these null alleles and analyzed growth at various temperatures (Table 3). The

Table 3. Growth profile of *CDC50/LEM3* and *DRS2/NEO1* family deletion mutants

Strains	18°C	25°C	30°C	37°C
Wild-type	+++	+++	+++	+++
*cdc50*Δ	−	+/−	+++	+++
*lem3*Δ	+++	+++	+++	+++
*drs2*Δ	−	+/−	+++	+++
*dnf1*Δ	+++	+++	+++	+++
*cdc50*Δ *drs2*Δ	−	+/−	+++	+++
*cdc50*Δ *dnf1*Δ	−	−	−	−
*cdc50*Δ *lem3*Δ	−	+/−	+	+
*drs2*Δ *dnf1*Δ	−	+/−	+	+
*drs2*Δ *lem3*Δ	−	−	−	−
*dnf1*Δ *lem3*Δ	+++	+++	+++	+++

Growth was examined on YPDA plates incubated at the temperatures indicated. Symbols indicate relative growth rate from wild-type (+++) to no growth (−). All double mutants were constructed by a cross followed by tetrad dissection.

*cdc50*Δ and *drs2*Δ mutants display similar growth phenotypes; both strains grew normally at 30°C or higher temperatures, grew slowly at 25°C, and did not grow at all at 18°C. Interestingly, both *cdc50*Δ *dnf1*Δ and *drs2*Δ *lem3*Δ double mutants exhibited synthetic growth defects. Furthermore, neither the *cdc50*Δ *drs2*Δ nor the *dnf1*Δ *lem3*Δ double mutants displayed reduced growth rates in comparison with respective single mutants. These results suggest that *DRS2* and *CDC50* perform similar functions, whereas *DNF1* and *LEM3* share similar gene functions, in spite of the lack of structural similarity between the *DRS2/NEO1* and *CDC50/LEM3* families.

*The drs2*Δ *Mutant Shows Defects in Polarized Growth*

As the *cdc50*Δ mutant exhibits defects in the establishment of cell polarity (Misu *et al*., 2003), we examined whether the *drs2*Δ mutant shows similar defects. *drs2*Δ mutant cells were grown at 18°C for 12 h as described previously (Misu *et al*., 2003) and analyzed for morphology and the distribution of filamentous actin. The *cdc50*Δ mutant cells exhibited a large and round morphology at 18°C (Figure 1A; Misu *et al*., 2003). *drs2*Δ mutant cells also were large and round at 18°C, although the magnitude of this effect was less pronounced than that seen in the *cdc50*Δ mutant (Figure 1A). Another morphological phenotype of *cdc50*Δ mutants is that *cdc50*Δ cells are arrested with small buds (Moir *et al*., 1982; Misu *et al*., 2003). The fraction of small-budded cells increased from 25% at 30°C to 40% after incubation at 18°C for 12 h (Misu *et al*., 2003). In contrast, no increase of small-budded cells could be observed for *drs2*Δ cells; when grown at either 18 or 30°C, *drs2*Δ mutant cell cultures contained 29 or 30% cells with small buds, respectively. Wild-type cells, in a manner similar to the *drs2*Δ mutant, contained 31% cells with small buds at both 18 and 30°C. *cdc50*Δ mutant cells also exhibited depolarization of cortical actin patches and defects in formation of actin cables (Misu *et al*., 2003). The depolarization of cortical actin patches could be observed in >90% of the small-budded *cdc50*Δ mutant cells at 18°C (Figure 1A; Misu *et al*., 2003). Staining of filamentous actin with phalloidin revealed that cortical actin patches were depolarized in 50% of the small-budded *drs2*Δ mutant cells at 18°C, in contrast to 8% of the wild-type cells with small buds (Figure 1A). When grown at 30°C, actin patches were depolarized in 13% of the small-budded *drs2*Δ mutant cells and only 4% of the

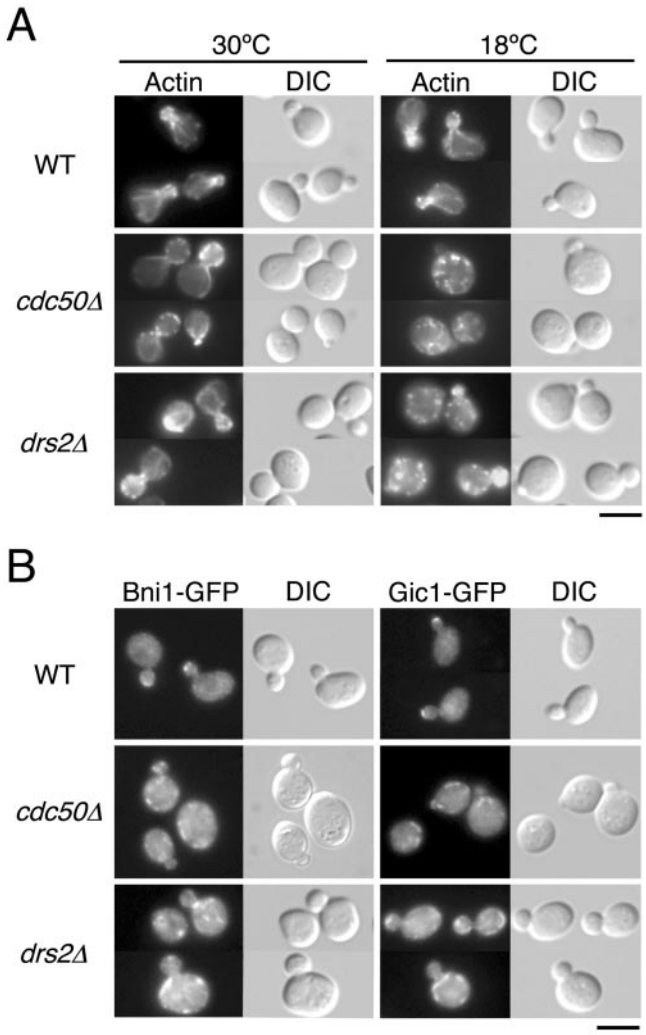

Figure 1. *drs2*Δ and *cdc50*Δ mutants exhibit defects in polarized growth. (A) Organization of the actin cytoskeleton in *drs2*Δ and *cdc50*Δ cells. Wild-type (YKT39), *cdc50*Δ (YKT249), and *drs2*Δ (YKT745) strains were grown in YPDA medium for 12 h at 18 or 30°C. After fixation, cells were stained with tetramethylrhodamine isothiocyanate-phalloidin and visualized by either DIC or epifluorescence. Bar, 5 μm. (B) Localization of GFP-tagged Bni1 and Gic1 proteins in *drs2*Δ and *cdc50*Δ cells. Cells were grown in YPDA medium for 12 h at 18°C and observed after fixation in 2% formaldehyde. The strains used were as follows: YKT455 (Bni1p-GFP in WT), YKT495 (Bni1p-GFP in *cdc50*Δ), YKT779 (Bni1p-GFP in *drs2*Δ), YKT579 (Gic1p-GFP in WT), YKT580 (Gic1p-GFP in *cdc50*Δ), and YKT781 (Gic1p-GFP in *drs2*Δ). Bar, 5 μm.

wild-type cells with small buds. Actin cables were absent from >95% of the small-budded *drs2*Δ mutant cells at 18°C, as well as *cdc50*Δ mutant cells (Figure 1A; Misu *et al*., 2003). At 30°C, actin cables were normally formed and polarized properly in >95% of the small-budded *drs2*Δ mutants and wild-type cells. These results suggest that the *drs2*Δ mutant is defective in the establishment of cell polarity, but exhibits less severe phenotypes than the *cdc50*Δ mutant.

Bni1p and Gic1p, regulators of polarized growth, are normally localized to growing sites, such as a bud tip or a cell division site. In the *cdc50*Δ mutant, both of these proteins were mislocalized at low temperatures (Misu *et al*., 2003). Mislocalization of Bni1p-GFP and Gic1p-GFP was observed in >95 and >80% of the small-budded *cdc50*Δ mutant cells at 18°C, respectively. We next examined the localization of these proteins in the small-budded *drs2*Δ mutant. A C-terminally GFP-tagged allele that we generated was integrated into the genome as the sole source of *BNI1* and *GIC1*. In the *drs2*Δ mutant grown at 18°C for 12 h, both Bni1p-GFP and Gic1p-GFP were mislocalized to punctate or tubular membranous structures, similar to those seen in the *cdc50*Δ mutant cells (Figure 1B). These Bni1p-GFP– and Gic1p-GFP–positive structures were often peripherally localized beneath the plasma membrane, but lacked polarized distributions. Mislocalization of Bni1p-GFP and Gic1p-GFP was seen in 68 and 50% of the small-budded *drs2*Δ mutant cells, respectively. These results suggest that Drs2p functions similarly to Cdc50p during polarized cell growth.

Cdc50p and Drs2p Are Localized to the TGN/Endosomal Membranes

We previously demonstrated that Cdc50p is localized to late endosomal/prevacuolar compartments (Misu *et al*., 2003). This study, however, also suggested that a fraction of Cdc50p may be localized to a compartment other than the late endosomal compartment. In contrast, Drs2p seemed to be colocalized with a TGN marker, Kex2p, by immunofluorescence microscopy (Hua *et al*., 2002). We examined the localization of Cdc50p to the TGN. To identify the TGN, we stained cells with another TGN marker, Sec7p (Franzusoff *et al*., 1991). We created diploid cells simultaneously expressing both a C-terminally GFP-tagged Cdc50p and a C-terminally mRFP1-tagged Sec7p to examine their distributions by fluorescence microscopy. Both Cdc50p-GFP and Sec7p-mRFP1 were observed as punctate structures scattered throughout the cell at 30°C (Figure 2A). Quantitative analysis of individual spots revealed that 57% of Cdc50p-GFP–positive structures were colocalized with Sec7p-mRFP1–positive structures (n = 315). Forty-eight percent of Sec7p-mRFP1-positive structures were colocalized with Cdc50p-GFP–positive structures (n = 371). We also introduced a C-terminally GFP-tagged Drs2p into diploid cells expressing Sec7p-mRFP1. Drs2p-GFP was colocalized with Sec7p-mRFP1 to a similar extent as that seen for the colocalization of Cdc50p with Sec7p (Figure 2A). Fifty-six percent of the Drs2p-GFP structures were colocalized with Sec7p-mRFP1 structures (n = 321). Conversely, 54% of Sec7p-mRFP1 structures were colocalized with Drs2p-GFP structures (n = 322), suggesting that both Cdc50p and Drs2p were localized to the TGN. To directly examine the colocalization of Cdc50p with Drs2p, we attempted to express an mRFP1-tagged Cdc50p; we failed, however, to detect Cdc50p-mRFP1 fluorescence, likely due to both the low fluorescence intensity of mRFP1 and the low expression levels for Cdc50p (our unpublished data).

We next examined whether Drs2p is also localized to late endosomal/prevacuolar compartments in a manner similar to Cdc50p. To facilitate detection of late endosomal/prevacuolar compartments, we examined the *vps27*Δ mutant strain. In *vps27*Δ cells, recycling Golgi proteins and endosomal proteins that traffic as far as the late endosome accumulate in a late endosomal/prevacuolar compartment, termed the class E compartment (Piper *et al*., 1995). FM4-64, a fluorescent membrane marker for endocytosis, also accumulates in the class E compartment of *vps27*Δ cells (Vida and Emr, 1995). *vps27*Δ mutant cells expressing Drs2p-GFP were loaded with FM4-64 dye, followed by a 30-min chase in fresh medium at 30°C. Similar to Cdc50p-GFP (Misu *et al*., 2003), a fraction of Drs2p-GFP was localized to the class E compartment labeled by FM4-64 (Figure 2B). Sec7p-GFP was not

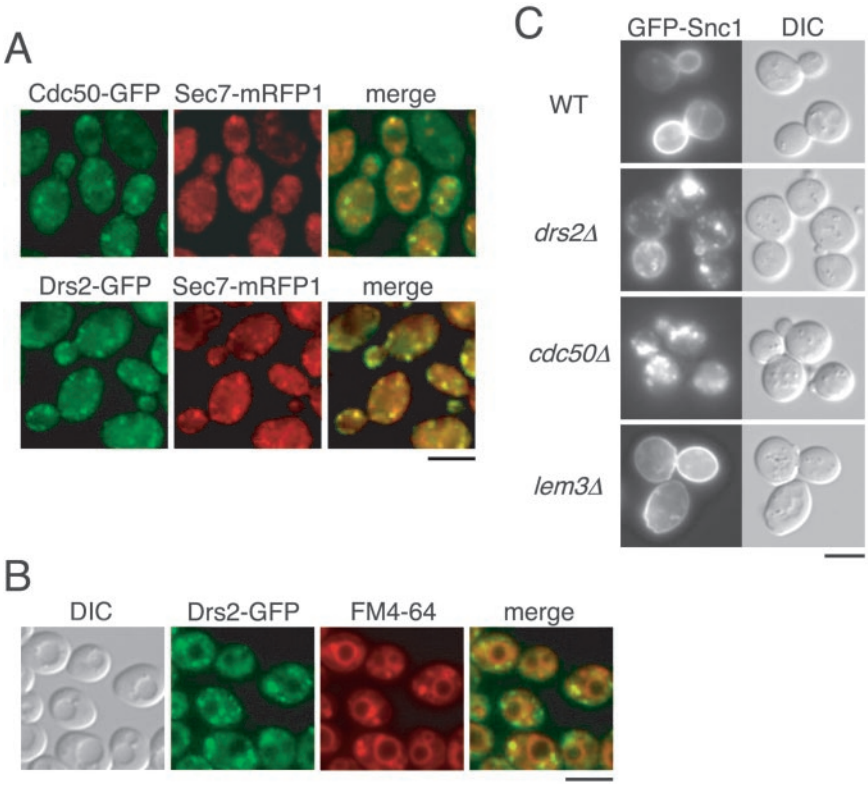

Figure 2. Cdc50p and Drs2p are localized to the TGN and endosomal membranes. (A) Colocalization of Cdc50p-GFP and Drs2p-GFP with mRFP1-tagged Sec7 protein. Wild-type cells expressing either *CDC50-GFP* (YKT788) or *DRS2-GFP* (YKT789) and *SEC7-mRFP1* were grown to early-mid logarithmic phase in YPDA medium at 30°C and observed after fixation in 1% formaldehyde. GFP- and mRFP1-tagged proteins were visualized using GFP (green) and G-2A (red) bandpass filters, respectively. Obtained images were merged to demonstrate the coincidence of the two signal patterns. Bar, 5 μm. (B) Accumulation of FM4-64 and Drs2p-GFP in the class E compartment of *vps27*Δ mutant cells. Cells expressing *DRS2-GFP* (YKT840) were grown to mid-late logarithmic phase in YPDA medium, labeled in 32 μM FM4-64 at 30°C for 15 min, and then chased in fresh medium at 30°C for 30 min. DIC images of the same cells were collected to visualize the vacuoles. FM4-64 and Drs2p-GFP images were acquired under the red and green fluorescence channels, respectively. A merged image of these two channels is also shown. Bar, 5 μm. (C) Localization of GFP-Snc1p in *drs2*Δ and *cdc50*Δ cells. pRS416 *GFP-SNC1* was introduced into YKT39 (WT), YKT745 (*drs2*Δ), YKT249 (*cdc50*Δ), and YKT496 (*lem3*Δ) strains. Cells were grown to early-mid logarithmic phase in SDA-Ura medium at 30°C and observed immediately by microscopy. GFP-tagged proteins were visualized using a GFP bandpass filter. Bar, 5 μm.

localized to the class E compartment in *vps27*Δ mutant cells (our unpublished data). Thus, both Cdc50p and Drs2p were distributed between the late endosome and the TGN. Hua *et al.* (2002) reported that *drs2*Δ mutant cells exhibit mislocalization of Snc1p, an exocytic v-SNARE protein (Gerst, 1997) that cycles between the cell surface and internal structures (Lewis *et al*., 2000). The mislocalization of GFP-Snc1p in the *drs2*Δ mutant may be explained by a defect in the exocytosis of proteins from the Golgi to the plasma membrane (Hua *et al*., 2002). We examined the involvement of Cdc50p in the recycling of GFP-Snc1p. In wild-type cells, although there was some internal fluorescence, GFP-Snc1p was observed primarily at the plasma membrane, concentrated within buds and regions of polarized growth (Figure 2C). In the *drs2*Δ mutant cells at 30°C, the amount of GFP-Snc1p localized to the plasma membrane decreased concomitant with an increase in the staining of internal punctate structures, which may be either the early endosome or the TGN (Hua *et al*., 2002). *cdc50*Δ mutant cells at 30°C exhibited a more severe defect in the mislocalization of GFP-Snc1p. GFP-Snc1p at the plasma membrane was faint; significant staining was only observed in the punctate structures (Figure 2C). GFP-Snc1p was localized normally in *lem3*Δ mutant cells at 30°C. These results suggest that both Cdc50p and Drs2p are involved in the recycling of GFP-Snc1p, possibly acting at the exocytic transport of Snc1p from the TGN to the plasma membrane (Hua *et al*., 2002).

Coimmunoprecipitation of Cdc50p/Lem3p Family with Drs2p/Neo1p Family

Our evidence that *cdc50*Δ and *drs2*Δ mutants are phenotypically similar and that both Cdc50p and Drs2p are localized to the TGN and late endosome raises the possibility that Cdc50p physically associates with Drs2p. We therefore attempted to isolate a complex of these proteins by coimmunoprecipitation experiments. We previously described a C-terminally HA-tagged version of *CDC50* that is functional (Misu *et al*., 2003). We also constructed and expressed a C-terminally Myc-tagged version of *DRS2* in cells expressing Cdc50p-HA. Drs2p-Myc was immunoprecipitated from membrane protein extracts prepared by solubilization in 1% CHAPS. Under our immunoprecipitation conditions, a TGN marker Kex2p was not precipitated nonspecifically (our unpublished data), indicating that Drs2p-Myc was efficiently solubilized from membranes. The resulting immunoprecipitates were analyzed by immunoblot by using both anti-Myc and anti-HA antibodies. Cdc50p-HA was coimmunoprecipitated with Drs2p-Myc (Figure 3A). Cdc50p-HA could not be detected in either control immunoprecipitates by using a nonspecific IgG (our unpublished data) or immunoprecipitates from cells lacking *DRS2-Myc* (Figure 3A). In addition, immunoprecipitation of Cdc50p-HA with an anti-HA antibody specifically isolated Drs2p-Myc (our unpublished data). These results indicate that the association of Cdc50p-HA with Drs2p-Myc is specific. In several immunoprecipitation experiments, ~10% of Drs2p-Myc was recovered from the lysate, and ~10–20% of Cdc50p-HA in the lysate was coimmunoprecipitated (our unpublished data). Therefore, we conclude that Cdc50p and Drs2p form a stable complex. When the blot was probed with anti-Lem3p antibodies, a small amount of Lem3p (<3% in the lysate) also could be detected in the immunoprecipitates from Drs2p-Myc–expressing cells. These results also suggest that a small fraction of Drs2p-Myc may associate with Lem3p.

The interaction between Cdc50p and Drs2p prompted us to examine a possible interaction between Lem3p and Dnf1p, because 1) the *lem3*Δ or *dnf1*Δ mutation does not affect cell growth, but they show synthetic lethal interaction with *cdc50*Δ and *drs2*Δ mutations; and 2) both Lem3p and Dnf1p are localized to the plasma membrane (Hua *et al*.,

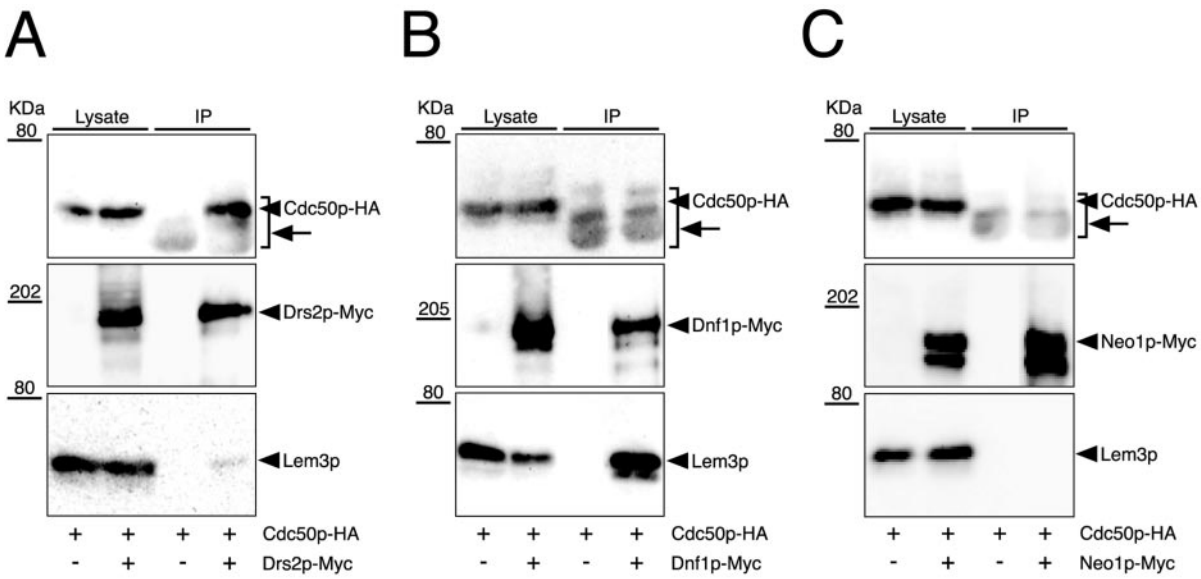

Figure 3. Coimmunoprecipitation of Cdc50p/Lem3p family members with Drs2p/Neo1p family members. Cells were grown at 25°C to a cell density of 0.5 OD_{600}/ml in YPDA medium. Membrane extracts were then prepared as described in the MATERIALS AND METHODS. Myc-tagged P-type ATPases were immunoprecipitated with an anti-Myc antibody from membrane extracts. Immunoprecipitates were subjected to SDS-PAGE, followed by immunoblot analysis using antibodies against HA (top), Myc (middle), and Lem3p (bottom). Arrows indicate the bands of anti-Myc antibody polypeptides detected by secondary antibodies (anti-mouse IgG-HRP). The results shown are representatives of several experiments. The strains used were as follows: YKT755 (Drs2p-Myc Cdc50p-HA) and YKT283 (Cdc50p-HA) (A), YKT759 (Dnf1p-Myc Cdc50p-HA) and YKT283 (Cdc50p-HA) (B), and YKT761 (Neo1p-Myc Cdc50p-HA) and YKT283 (Cdc50p-HA) (C).

2002; Kato *et al*., 2002; Hanson *et al*., 2003; Pomorski *et al*., 2003). We constructed and introduced a C-terminally Myc-tagged version of *DNF1* into cells. Immunoprecipitation of Dnf1p-Myc with an anti-Myc antibody coimmunoprecipitated Lem3p (Figure 3B). In several immunoprecipitation experiments, ~10% of Dnf1p-Myc was recovered from the lysate, and ~20% of Lem3p in the lysate was coimmunoprecipitated (our unpublished data). Cdc50p-HA was not detectable in these immunoprecipitates, suggesting specificity of the interaction between Dnf1p and Lem3p. We immunoprecipitated Neo1p-Myc, which possesses a function unique among the members of the *DRS2/NEO1* family. Neither Cdc50p-HA nor Lem3p was detectable in the immunoprecipitates (Figure 3C), suggesting that Neo1p does not associate with either Cdc50p or Lem3p. These data demonstrate that Cdc50p forms a complex with Drs2p, whereas Lem3p forms a complex with Dnf1p in vivo.

Association of Cdc50p with Drs2p Is Required for the ER Exit of the Cdc50p-Drs2p Complex

To elucidate the function of Cdc50p interaction with Drs2p, we examined the localization of Drs2p-GFP in the absence of Cdc50p by fluorescence microscopy. In the *cdc50*Δ mutant at 30°C, Drs2p-GFP occurred within typical endoplasmic reticulum (ER) structures in yeast, which morphologically envelop the nucleus and extend from perinuclear membranes that frequently reach the periphery of the cell proximal to the plasma membrane (Figure 4A). Costaining with 4,6-diamidino-2-phenylindole dye confirmed that the Drs2p-GFP–positive structures in the *cdc50*Δ mutant were perinuclear (our unpublished observation). These results suggest that Drs2p-GFP could not be transported out of the ER in the absence of Cdc50p. In the *lem3*Δ mutant at 30°C, Drs2p-GFP occurred within punctate structures scattered throughout the cell, as is seen in wild-type cells. We next examined whether the absence of Lem3p would have a similar effect on the localization of Dnf1p. A C-terminally GFP-tagged allele of *DNF1* was generated and integrated into the yeast genome to be the sole source of *DNF1*. Dnf1p-GFP in wild type was found in internal membranes and small punctate structures underlying the plasma membrane, concentrated at sites of emerging buds, small buds, and the mother-daughter neck of dividing cells (Hua *et al*., 2002; Pomorski *et al*., 2003). Dnf1p-GFP occurred within typical ER structures in the *lem3*Δ mutant at 30°C but not in the *cdc50*Δ mutant (Figure 4A). In the absence of Cdc50p, the amount of Dnf1p-GFP localized to sites of polarization diminished in most cells even at 30°C, likely due to the defects in cell polarization resulting from the *cdc50*Δ mutation. The localization of Neo1p-GFP in the *cdc50*Δ mutant at 30°C did not differ from that seen in wild-type cells; Neo1p-GFP occurred in ER-like structures and in several peripheral punctate structures, some of which were associated with the ER (Figure 4A; Hua and Graham, 2003). These results indicate that Cdc50p and Lem3p are required for the ER exit of Drs2p and Dnf1p, respectively. In the *drs2*Δ mutant at 30°C, Cdc50p-GFP was also mislocalized (Figure 4B), suggesting that the stable association of Drs2p with Cdc50p within the ER is essential for the ER exit of the Cdc50p-Drs2p complex. To substantiate this conclusion, we examined the complex formation within the ER by using a temperature-sensitive *sec12-4* mutant, in which the vesicle transport from the ER to the Golgi is blocked. Drs2p-Myc was immunoprecipitated in *sec12-4* mutant incubated at 35°C for 1 h. Under these conditions, Cdc50p-GFP was confined within the ER (our unpublished observation). Cdc50p-HA was coimmunoprecipitated with Drs2p-Myc, and similarly, Lem3p was coimmunoprecipitated with Dnf1p-Myc (Figure 4C), indicating that the Drs2p-Cdc50p and Dnf1p-Lem3p complexes are formed within the ER.

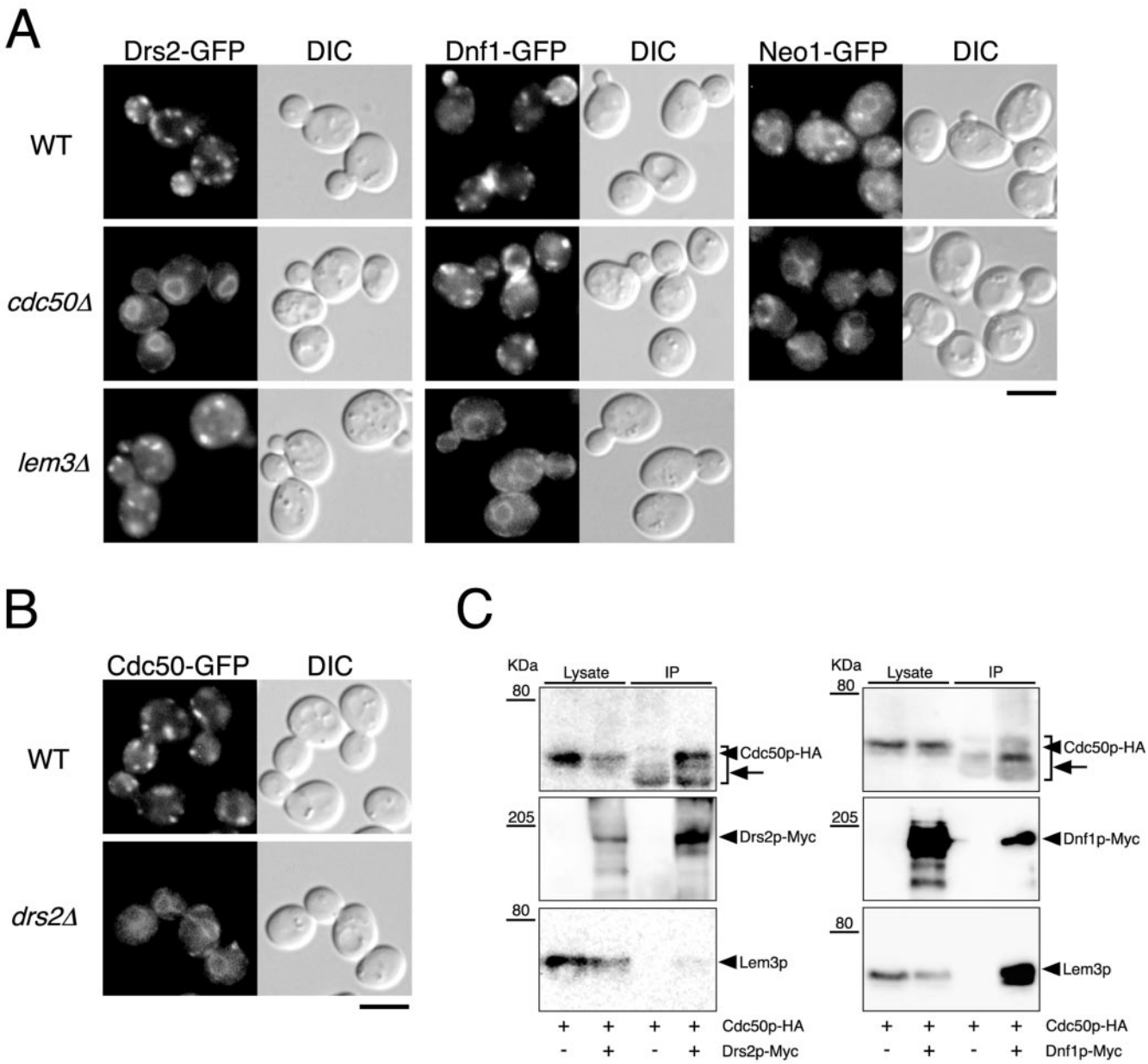

Figure 4. Cdc50p-Drs2p and Lem3p-Dnf1p complex formation is required for the ER exit of these proteins. (A) Localization of Drs2p-GFP, Dnf1p-GFP, and Neo1p-GFP in wild-type, *cdc50*Δ, and *lem3*Δ cells. (B) Localization of Cdc50p-GFP in wild-type and *drs2*Δ cells. Cells were grown to early-mid logarithmic phase in YPDA medium at 30°C and observed immediately by microscopy. GFP-tagged proteins were visualized using a GFP bandpass filter. The strains used were as follows: YKT768 (Drs2p-GFP in WT), YKT769 (Drs2p-GFP in *cdc50*Δ), YKT770 (Drs2p-GFP in *lem3*Δ), YKT771 (Dnf1p-GFP in WT), YKT772 (Dnf1p-GFP in *cdc50*Δ), YKT773 (Dnf1p-GFP in *lem3*Δ), YKT775 (Neo1p-GFP in WT), YKT776 (Neo1p-GFP in *cdc50*Δ), YKT259 (Cdc50p-GFP in WT), YKT774 (Cdc50p-GFP in *drs2*Δ). Bars, 5 μm. (C) Coimmunoprecipitation of Cdc50p and Lem3p with Drs2 and Dnf1p, respectively, in *sec12-4* cells. *sec12-4* cells were grown at 25°C to mid logarithmic phase in YPDA medium and then incubated at 35°C for 1 h. Drs2p-Myc or Dnf1p-Myc was immunoprecipitated with anti-Myc antibody, and the precipitated proteins were detected by immunoblot analysis as described for Figure 3. Arrows indicate anti-Myc antibody detected by secondary antibodies (anti-mouse IgG-HRP). The strains used were as follows: YKT913 (Drs2p-Myc Cdc50p-HA *sec12-4*), YKT914 (Dnf1p-Myc Cdc50p-HA *sec12-4*), and YKT915 (Cdc50p-HA *sec12-4*).

A C-terminally HA-tagged Lem3p was not fully functional, as *cdc50*Δ strains expressing *LEM3-HA* as a sole source of *LEM3* exhibited a growth defect at 30°C, a permissive temperature for the parental *cdc50*Δ mutant (Figure 5A). Indirect immunofluorescence microscopy by using an anti-HA antibody revealed that Lem3p-HA was localized to internal membranes and small punctate structures underlying the plasma membrane concentrated at sites of polarized growth (Figure 5B), suggesting that Lem3p-HA transports normally out of the ER to the plasma membrane. Reinforcing this possibility, Dnf1p-GFP in *LEM3-HA* cells was localized properly to the plasma membrane at sites of polarization as observed in wild-type cells (Figure 5C). Lem3p-HA also was coimmu-

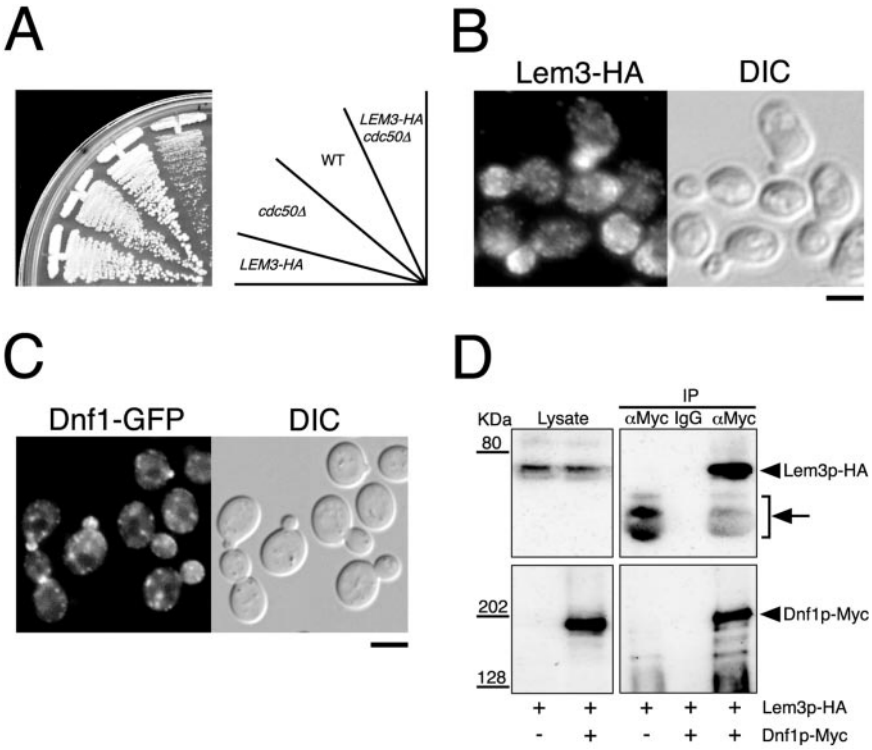

Figure 5. Function and localization of a C-terminally HA-tagged Lem3 protein. (A) Growth defect of *cdc50*Δ mutant strains expressing Lem3p-HA. A tetra type tetrad from a diploid cell, heterozygous for *LEM3-HA* and *cdc50*Δ, was grown at 30°C. After streaking, YPDA plates were incubated at 30°C for 2 d. The result shown is representative of 10 independent tetrads. (B) Indirect immunofluorescence of Lem3p-HA. Cells expressing Lem3p-HA (YKT782) were prepared for immunofluorescence as described in MATERIALS AND METHODS. Cells were stained with an anti-HA antibody. Bar, 5 μm. (C) Localization of GFP-tagged Dnf1 protein in cells expressing Lem3p-HA. Cells expressing Dnf1p-GFP and Lem3p-HA (YKT809) were grown to early-mid logarithmic phase in YPDA medium at 30°C and observed immediately by microscopy. Bar, 5 μm. (D) Coimmunoprecipitation of Lem3p-HA with Dnf1p-Myc. Cells were grown at 25°C to a cell density of 0.5 OD_{600}/ml in YPDA medium. Extracts prepared from YKT807 (Lem3p-HA Dnf1p-Myc) or YKT808 (Lem3p-HA) cells were subjected to immunoprecipitation with either an anti-Myc antibody or control mouse IgG. Immunoprecipitates were subjected to SDS-PAGE, followed by immunoblot analysis by using antibodies against HA (top) and Myc (bottom). An arrow indicates anti-Myc antibody detected by secondary antibodies (anti-mouse IgG-HRP).

noprecipitated with Dnf1p-Myc (Figure 5D), indicating that Lem3p-HA forms a complex with Dnf1p-Myc within the ER, which is normally transported out of the ER. Lem3p likely plays an additional important role within the mature Lem3p-Dnf1p complex, after it has reached sites of polarization, which is independent from its structural role in the ER exit of the Lem3p-Dnf1p complex.

Drs2p and Cdc50p Seem to Cycle between the TGN and Plasma Membrane

The distinct subcellular localizations of Cdc50p-Drs2p and Lem3p-Dnf1p raise the question of how these molecular complexes can perform redundant functions. Hua *et al.* (2002) proposed that if Dnf1p cycles between the exocytic and endocytic pathways, it could be a transient occupant of the TGN. We hypothesize that Cdc50p-Drs2p also may cycle between the TGN and plasma membrane, possibly substituting for the function of Lem3p-Dnf1p at the plasma membrane. We examined the localization of Drs2p-GFP in a mutant of *VRP1*, a protein required for proper organization of cortical actin patches and the internalization step during endocytosis (Munn *et al.*, 1995). Drs2p-GFP, which was barely detectable at the plasma membrane in wild-type cells, could be seen at the plasma membrane in the *vrp1*Δ mutant cells at 25°C (Figure 6), indicating that Drs2p is transported to the plasma membrane. This increased staining at the cell surface occurred concomitant with a reduction in the intensity of Drs2p-GFP intracellular staining. Similar results were obtained for Cdc50p-GFP (Figure 6), suggesting that the Cdc50p-Drs2p complex recycles between the TGN and plasma membrane. To confirm that Dnf1p cycles between the plasma membrane and internal membranes underlying the plasma membrane, we examined the localization of Dnf1p-GFP in *vrp1*Δ mutant cells at 25°C. The majority of Dnf1p-GFP staining in *vrp1*Δ mutant cells was localized to the plasma membrane, becoming only barely detectable on smaller punctate structures, indicating that Dnf1p also cycles between those membranes (Figure 6). These results suggest that Drs2p and Dnf1p cycles between the plasma membrane and internal membranes, such as the endosome

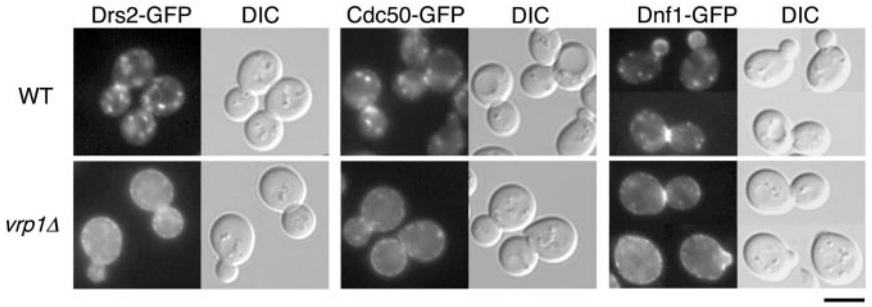

Figure 6. Localization of GFP-tagged Drs2, Cdc50, and Dnf1 proteins in *vrp1*Δ cells. Wild-type and *vrp1*Δ cells expressing either *DRS2-GFP*, *CDC50-GFP*, or *DNF1-GFP* were grown to early-mid logarithmic phase in YPDA medium at 25°C and observed immediately by microscopy. GFP-tagged proteins were visualized using a GFP bandpass filter. The strains used were as follows: YKT768 (Drs2p-GFP in WT), YKT777 (Drs2p-GFP in *vrp1*Δ), YKT259 (Cdc50p-GFP in WT), YKT834 (Cdc50p-GFP in *vrp1*Δ), YKT771 (Dnf1p-GFP in WT), YKT804 (Dnf1p-GFP in *vrp1*Δ). Bar, 5 μm.

A

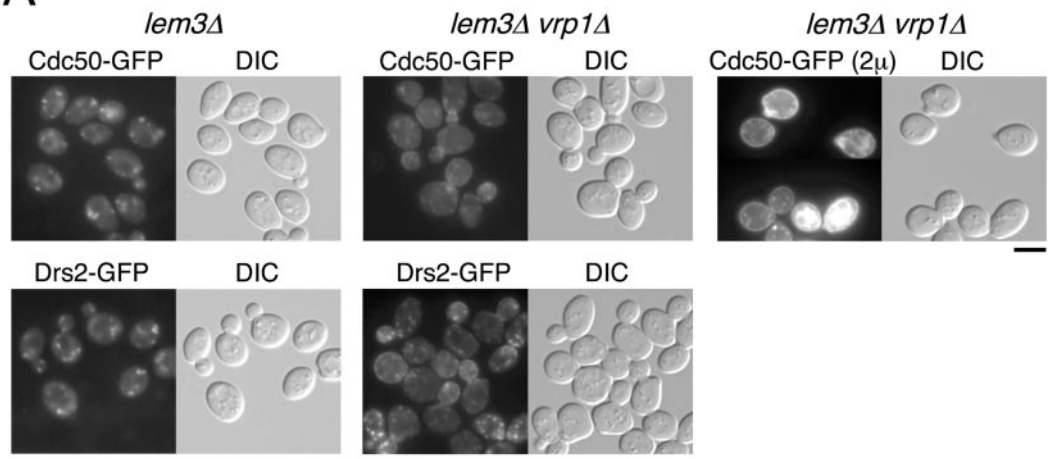

B

Strains		Fluorescence (% of wild type)		
		NBD-PE	NBD-PC	NBD-PS
WT	+ YEplac195	100	100	100
lem3Δ	+ YEplac195	46.0±7.4	16.8±4.2	158.2±32.2
lem3Δ vrp1Δ	+ YEplac195	92.4±5.8	36.9±4.8	283.1±22.8
lem3Δ vrp1Δ	+ YEplac195 DRS2-CDC50	130.3±27.3	49.4±10.5	342.9±36.0

Figure 7. Localization of GFP-tagged Drs2 and Cdc50 proteins and the accumulation of NBD-labeled phospholipids in *lem3*Δ and *lem3*Δ *vrp1*Δ cells. (A) Localization of Cdc50p-GFP and Drs2p-GFP in *lem3*Δ and *lem3*Δ *vrp1*Δ cells. The *lem3*Δ (left column) and *lem3*Δ *vrp1*Δ (middle column) cells expressing either *CDC50-GFP* or *DRS2-GFP* were grown to early to mid logarithmic phase in YPDA medium at 25°C and observed immediately by microscopy. The *lem3*Δ *vrp1*Δ cells harboring both pKT1266 (YEplac181 *CDC50-EGFP*) and pKT1468 (YEplac195 *DRS2*) (right column) were grown to early-mid logarithmic phase in SD-Leu-Ura medium at 25°C and observed immediately by microscopy. GFP-tagged proteins were visualized using a GFP bandpass filter. For observation of each image, the same exposure and processing parameters were used. The strains used were as follows: YKT836 (Cdc50p-GFP in *lem3*Δ), YKT770 (Drs2p-GFP in *lem3*Δ), YKT805 (Cdc50p-GFP in *lem3*Δ *vrp1*Δ), YKT806 (Drs2p-GFP in *lem3*Δ *vrp1*Δ), and YKT843 (*lem3*Δ *vrp1*Δ) harboring pKT1266 and pKT1468. Bar, 5 μm. (B) Percentage of accumulation of NBD-labeled phospholipids of the deletion mutants relative to wild-type cells. pKT1472 (YEplac195 *DRS2 CDC50*) was introduced into YKT839 (*lem3*Δ *vrp1*Δ) strain. YEplac195 was introduced into YKT39 (WT), YKT496 (*lem3*Δ), and YKT839 (*lem3*Δ *vrp1*Δ) strains. Cells carrying the appropriate plasmids were grown to early-mid logarithmic phase in SD-Ura medium at 25°C and labeled with either NBD-PE, -PC, or -PS for 30 min at 25°C. The percentage of average accumulation for the deletion mutants relative to wild-type cell is presented with ±SD of seven independent experiments.

and TGN, so that either pair can substitute for the function of the other.

Drs2p May Regulate the Translocation of NBD-labeled Phosphatidylethanolamine and Phosphatidylserine

Whereas the *drs2*Δ mutant exhibits defects in APT activity at the plasma membrane (Tang *et al*., 1996; Gomes *et al*., 2000), this result remains under dispute (Siegmund *et al*., 1998; Marx *et al*., 1999). Because Drs2p was localized to the TGN, it is difficult to detect its APT activity at the plasma membrane in wild-type cells. Cdc50p-Drs2p becomes confined to the plasma membrane, however, when endocytosis is blocked by mutations in *VRP1*. Kato *et al.* (2002) and Hanson *et al.* (2003) have reported that the *lem3*Δ mutant has a defect in the transport of NBD-PE and -PC across the plasma membrane. Therefore, it remains possible that, in the *lem3*Δ *vrp1*Δ mutant, we may be able to detect lipid transport activity of Cdc50p-Drs2p accumulated to the plasma membrane. Drs2p-GFP and Cdc50p-GFP were localized to the plasma membrane in *lem3*Δ *vrp1*Δ mutant cells at 25°C (Figure 7A), although the intracellular punctate staining became more intense than that seen in *vrp1*Δ mutant cells (Figure 6). The plasma membrane localization of Drs2p-GFP and Cdc50p-GFP was distinctly evident when these cells were compared with the *lem3*Δ mutant (Figure 7A).

After cell labeling with either NBD-PE, -PC, or -PS, we determined the average cell-associated NBD fluorescence per cell by flow cytometry as described previously (Siegmund *et al*., 1998). Fluorescent lipid accumulation was measured for wild-type, *lem3*Δ, and *lem3*Δ *vrp1*Δ cells grown at 25°C in SD medium. Calculation of the cell-associated fluorescence in the mutants, expressed as a percentage of that seen for wild-type cells (Figure 7B) revealed that the uptake of NBD-PE in the *lem3*Δ mutant decreased to 46% that of the wild-type. In the *lem3*Δ *vrp1*Δ mutant, NBD-PE uptake was restored to 92% that of the wild-type, suggesting that

Cdc50p-Drs2p is also involved in NBD-PE internalization. The uptake of NBD-PC in the *lem3*Δ mutant decreased to 17% of that seen in the wild-type. In the *lem3*Δ *vrp1*Δ double mutant, NBD-PC internalization was minimally restored to levels 37% that of the wild-type, suggesting that Cdc50p-Drs2p is weakly involved in NBD-PC internalization. Interestingly, the uptake of NBD-PS in the *lem3*Δ mutant was increased to 158% that of the wild-type. In the *lem3*Δ *vrp1*Δ mutant, NBD-PS uptake increased to 283% that of the wild-type, suggesting the strong involvement of Cdc50p-Drs2p in NBD-PS internalization. These results suggest that Cdc50p–Drs2p possesses an APT activity; we cannot, however, exclude the possibility that additional proteins localized to the plasma membrane upon Vrp1p deficiency contribute to increases in the uptake of NBD-PE, -PC, and -PS in the *lem3*Δ *vrp1*Δ mutant. To confirm that Cdc50p-Drs2p is responsible for the increased uptake of NBD-labeled phospholipids in the *lem3*Δ *vrp1*Δ mutant, we attempted to construct both a *lem3*Δ *vrp1*Δ *drs2*Δ and a *lem3*Δ *vrp1*Δ *cdc50*Δ mutant. The *vrp1*Δ mutation results in synthetic lethality when combined with *drs2*Δ and *cdc50*Δ mutations (our unpublished data). We examined the uptake of NBD-labeled phospholipids in *lem3*Δ *vrp1*Δ cells overexpressing both *DRS2* and *CDC50*. When Cdc50p-GFP and Drs2p were overexpressed in *lem3*Δ *vrp1*Δ mutant cells, stronger GFP signals were observed at the plasma membrane than in the parental strain (compare top middle panel with top right panel in Figure 7A). Overexpression of Cdc50p and Drs2p markedly enhanced NBD-PE and NBD-PS uptake to 130 and 343% of wild-type levels, respectively, and minimally increased the incorporation of NBD-PC to 49% of wild-type levels (Figure 7B). These results suggest that the Cdc50p-Drs2p complex possesses APT activity, which translocates aminophospholipids more efficiently than PC.

DISCUSSION

Cdc50p and Lem3p Are Potential β-Subunits of Phospholipid-translocating P-Type ATPases

In this work, we demonstrate that Cdc50p and Lem3p associate with members of APT subfamily of the P-type ATPases. The assembly of Drs2p with Cdc50p on the ER membrane is essential for the ER exit of the Cdc50p-Drs2p complex. Similar observations have been made for the vertebrate plasma membrane Na^+, K^+-ATPase, another P-type ATPase consisting of a catalytic α-subunit and a noncatalytic β-subunit. Assembly of the complex occurs in the ER; the α- and β-subunits are mutually dependent for transport out of the ER (Geering, 1990). Unassembled α- and β-subunits seem to be retained in the ER through the action of the ER quality control machinery (Beggah *et al*., 1996). They showed that unassembled β-subunits associate with BiP, a chaperone in the ER, until assembly with α-subunits occurs. Another type of quality control mechanism was reported for the ER retention of unassembled subunit (Fet3p) of a yeast iron transporter (Sato *et al*., 2004). In this case, unassembled Fet3p is transported out of the ER but retrieved from the Golgi through Rer1p, a retrieval receptor for ER-resident membrane proteins in the Golgi. Similar mechanisms may operate to retain unassembled subunits of phospholipid translocating P-type ATPases in the ER in yeast.

The β-subunit is likely required for the regulation of the Na^+, K^+-pump transport activity of the mature complex (Geering *et al*., 1996). Therefore, the Na^+, K^+-ATPase ER assembly process establishes not only the basic structural interactions between the subunits, required for maturation of the oligomeric proteins, but also distinct, functional interactions involved in the regulation of mature protein's functional properties. HA-tagged Lem3p was transported normally to the cell surface in a form complexed with Dnf1p. This *LEM3-HA* exhibited a weak synthetic growth defect with the *cdc50*Δ mutation, suggesting that Lem3p performs a function in the mature Lem3p-Dnf1p complex that cannot be performed by the HA-tagged form after reaching the plasma membrane. Lem3p also may be involved in the regulation or activation of the catalytic activity of Dnf1p, as occurs for the β-subunit of Na^+, K^+-ATPase.

Because the Cdc50/Lem3 family of proteins are conserved throughout evolution (Misu *et al*., 2003), it would be interesting to investigate whether a Cdc50 family protein associates with a P-type ATPase in other organisms. A phospholipid-translocating ATPase, however, may not associate with a Cdc50p/Lem3p-related protein. Neo1p did not associate with either Cdc50p or Lem3p by coimmunoprecipitation. Neo1p may associate with Crf1p; this protein is dispensable for cell growth, indicating that Crf1p is not required for the full function of Neo1p. Neo1p may associate with a different type of membrane protein or function without stable association with other proteins. Neo1p has recently been shown to be required for retrograde transport from the Golgi to the ER (Hua and Graham, 2003). A temperature-sensitive *neo1* mutation exhibited a synthetic lethality with the *drs2*Δ mutation. This result, combined with our result that overexpression of *NEO1* suppresses the cold-sensitive growth phenotype of the *cdc50*Δ mutant, suggests a functional overlap between Neo1p and Cdc50p-Drs2p. As hypothesized by Hua and Graham (2003), both Neo1p and Drs2p may maintain lipid asymmetry throughout the Golgi network, with Neo1p acting within the *cis* compartment and Drs2p in the *trans*. It is interesting, however, that Neo1p is regulated in a manner different from that of Drs2p and Dnf1p.

Coimmunoprecipitation experiments suggested that a fraction of Lem3p associated with Drs2p. Overexpression of *LEM3* efficiently suppressed the cold-sensitive growth defect of the *cdc50*Δ mutant, but it did not alter the growth of the *drs2*Δ mutant (our unpublished data). This result suggests that *LEM3* overexpression requires *DRS2* to be present to suppress defects resulting from Cdc50p deficiency. Therefore, the interaction of Lem3p with Drs2p may be functionally significant. Lem3p also may interact with Dnf2p, a homolog of Dnf1p (83% similar and 69% identical at the amino acid level) (Hua *et al*., 2002). This assumption is supported by the observations that Dnf1p and Dnf2p exhibit redundant activities in phospholipid translocation across the plasma membrane (Pomorski *et al*., 2003), whereas the *lem3*Δ mutation alone is sufficient to cause severe defects in phospholipid translocation (Kato *et al*., 2002; Hanson *et al*., 2003). Two recent reports have suggested that Lem3p-GFP is localized to the ER as well as the plasma membrane (Kato *et al*., 2002; Hanson *et al*., 2003). We also observed ER localization of a C-terminally GFP-tagged Lem3p when expressed from the *LEM3* genomic locus under the control of the native promoter (our unpublished data). Lem3p-GFP does not seem to be functional, because *LEM3-GFP* exhibited a severe synthetic growth defect with the *cdc50*Δ mutation (our unpublished data); *LEM3-GFP* strains also do not internalize NBD-labeled PC (Hanson *et al*., 2003). Therefore, Lem3p-GFP observed in the ER seems to be incapable of forming a complex with Dnf1p, remaining in the ER due to a failure of ER exit. Because an HA-tagged Lem3p was also not fully functional, the C terminus of Lem3p may mediate critical functions.

The Cdc50p-Drs2p Complex Functions at Multiple Sites

In wild-type cells, the Cdc50p-Drs2p complex is localized to the TGN and late endosome. Our results suggested that the Cdc50p-Drs2p complex reaches the plasma membrane, but it is actively cleared by endocytosis. In the *vrp1*Δ mutant, the punctate localization of Cdc50p-GFP and Drs2p-GFP was no longer observable, suggesting that the Cdc50p-Drs2p complex is rapidly recycled from the plasma membrane to achieve a steady-state localization at the TGN. *vrp1*Δ mutant strains grow normally at 18°C, a nonpermissive temperature for the *cdc50*Δ and *drs2*Δ mutants (our unpublished data), suggesting that Cdc50p-Drs2p is not required to be exclusively localized within the TGN to perform its essential function; both Cdc50p-GFP and Drs2p-GFP were in fact mislocalized to the plasma membrane in the *vrp1*Δ mutant at 18°C (our unpublished observation). Because Lem3p-Dnf1p, a complex that shares redundant functions in cell growth with Cdc50p-Drs2p, is localized primarily to the plasma membrane (Pomorski *et al*., 2003), Cdc50p-Drs2p also may function at the plasma membrane. One such function seems to be in the internalization step during endocytosis; the *dnf1*Δ *dnf2*Δ *drs2*Δ mutant strain, but not the *dnf1*Δ *dnf2*Δ or *drs2*Δ mutants, displays a defect in endocytosis at 15°C (Pomorski *et al*., 2003). Therefore, Cdc50p-Drs2p, implicated in the formation of CCVs at TGN membranes (Chen *et al*., 1999), seems to function in vesicular trafficking at multiple cellular sites.

We first isolated *CDC50* as a multicopy suppressor of the temperature-sensitive growth defect of *myo3*Δ *myo5-360* mutant (Misu *et al*., 2003). We also observed a similar growth suppression of *myo3*Δ *myo5-360* by multicopy *DRS2* (our unpublished data). Myo3p and Myo5p are required for the internalization step of endocytosis as a factor that assembles cortical actin patches (Geli and Riezman, 1998). The *myo5-360* mutation causes two amino acid substitutions, K972G and S1005P, both in the tail region of Myo5p (Fujimura-Kamada and Tanaka, unpublished data). Interestingly, the basic tail region of type I myosins interacts with acidic phospholipids (Tang *et al*., 2002). Specific changes of phospholipid composition in the plasma membrane bilayer may regulate the function of Myo5p.

Dnf1p is localized to regions of polarization at the plasma membrane, including bud tips and sites of cell division. Dnf1p is also localized to intracellular structures, which are partially colocalized with a TGN marker Kex2p (Hua *et al*., 2002). In *vrp1*Δ mutant cells, Dnf1p-GFP was localized primarily to the plasma membrane, losing its intracellular localization, suggesting that Dnf1p also may be recycled by endocytosis. Snc1p, a v-SNARE protein recycled for vesicle fusion became trapped in intracellular structures in both the *cdc50*Δ mutant (Figure 2C) and the *drs2*Δ mutant (Hua *et al*., 2002). Similarly, in *cdc50*Δ mutant cells grown at 18°C, Dnf1p was observed in intracellular punctate structures, not at the cell periphery (our unpublished observation). Previous observations that phospholipid-translocation was diminished in the *drs2*Δ mutant (Tang *et al*., 1996) may result from the entrapment of Lem3p-Dnf1p in intracellular spaces. The degree of entrapment would be affected by various factors, such as the preincubation temperature, incubation time before assay, and strain background, possibly explaining the controversial observations reported (Siegmund *et al*., 1998; Marx *et al*., 1999).

Cdc50p-Drs2p Seems to Function as an Aminophospholipid Translocase

Because Cdc50p-Drs2p is localized to the TGN, it is not possible to examine APT activity of Cdc50p-Drs2p by measuring the uptake of NBD-labeled phospholipids across the plasma membrane. The altered localization of Cdc50p-Drs2p to the plasma membrane in a mutant defective for endocytosis, however, enabled us to examine the APT activity of Cdc50p-Drs2p in the absence of Lem3p. We observed a significant increase in the uptake of NBD-labeled aminophospholipids in the *lem3*Δ *vrp1*Δ mutant, in comparison with the *lem3*Δ mutant. This increase was enhanced by the overexpression of *CDC50* and *DRS2*. The increases in the uptake were more prominent for PS and PE than for PC, suggesting that Drs2p possesses an APT activity. Interestingly, *lem3*Δ mutant cells are defective in the uptake of NBD-PC and NBD-PE, but not of NBD-PS (Figure 7; Kato *et al*., 2002; Hanson *et al*., 2003). These results may reflect different substrate specificities of Drs2p and Dnf1p; Drs2p may have a higher activity against PS and PE, whereas Dnf1p may have a higher specificity toward PC and PE.

The phospholipid asymmetry generated by Drs2p APT activity seems to drive the formation of vesicles. Chen *et al*. (1999) demonstrated that *drs2*Δ cells exhibited a marked reduction in the number of CCVs that could be isolated. Drs2p plays a role in the budding of adaptor protein complex-3–coated vesicles carrying alkaline phosphatase to the vacuole (Hua *et al*., 2002). Various observations have suggested the importance of phospholipid asymmetry in the formation of vesicles. PE or PS added exogenously to the outer leaflet of the plasma membrane could be translocated into the inner leaflet and enhanced endocytosis (Farge *et al*., 1999). Transbilayer movement of lipids may induce the bending of membranes to facilitate vesicle budding (Devaux, 1991); indeed, induced bilayer asymmetry can convert spherical liposomes into tubular and interconnected vesicular structures (Farge and Devaux, 1992). Aminophospholipids translocated into the cytoplasmic leaflet may also recruit proteins for vesicle budding; clathrin can be recruited on chemically defined liposomes, but the production of clathrin-coated buds on the membranes requires a high concentration of PE (40% of total lipid) (Takei *et al*., 1998). The PS concentration may also affect the association of ARF guanine nucleotide exchange factors with Golgi membranes (Chardin *et al*., 1996). In vitro studies using membranes isolated from *drs2*Δ cells would facilitate clarifying regulatory role of phospholipid asymmetry in vesicle formation.

Roles of Cdc50p-Drs2p for Polarized Growth

The *drs2*Δ mutant exhibited less severe defects than the *cdc50*Δ mutant in not only cell polarity but also localization of GFP-Snc1p, suggesting that Cdc50p may possess an additional function independent of its role as a Drs2p-interacting protein. Cdc50p may interact with another P-type ATPase, a candidate for which is Dnf3p. Dnf3p is localized to punctate intracellular structures, reminiscent of Drs2p localization (Hua *et al*., 2002). Mislocalization of polarity regulators, Bni1p and Gic1p, may account for the defects in cell polarity of both the *cdc50*Δ and *drs2*Δ mutants. It remains to be determined, however, whether Cdc50p-Drs2p activity is required for the maintenance of Bni1p and Gic1p at sites of polarization, or for the polarized transport of Bni1p and Gic1p. In the former case, a subpopulation of Cdc50p-Drs2p localized at the plasma membrane may create a favorable lipid environment for the maintenance of polarity regulators. Because both Bni1p and Gic1p are effectors of the Cdc42p small GTPase, localization of Bni1p and Gic1p may be dependent on Cdc42p. Cdc42p is anchored to membranes through a prenylation site at its C terminus. It will be interesting to determine whether the phospholipid composition of the plasma membrane can regulate the polarized localization of Cdc42p. Generation of phospholipid asymmetry within a spe-

cific region of the plasma membrane has been implicated in the cytokinesis of mammalian cells (Emoto and Umeda, 2000). PE may be exposed to the outer leaflet of the plasma membrane at the cleavage furrow; subsequent redistribution of this PE is required for the disassembly of the contractile apparatus.

In the latter case, polarity regulators may be transported to sites of polarization by vesicles whose formation is dependent on Cdc50p-Drs2p activity. Bud6p/Aip3p, an actin-binding protein that also interacts with Bni1p, is transported to the polarized sites through the conventional secretory pathway (Jin and Amberg, 2000). Bni1p, however, is not dependent on the conventional secretory pathway for transport (Jin and Amberg, 2000). Polarized transport of Cdc42p is dependent on a type V myosin Myo2p (Wedlich-Soldner *et al*., 2003), suggesting that a Cdc42p-containing transport vesicle may be cargo for Myo2p. In *drs2*Δ mutant cells, the secretion of pro-α-factor is not severely compromised at 15°C (Chen *et al*., 1999), despite the inhibition of cell growth at this temperature. Thus, there may be a specific class of vesicles specifically involved in polarized growth; Cdc50p–Drs2p may regulate the formation of such secretory vesicles.

The third possibility has recently been reported (Valdez-Taubas and Pelham, 2003). In this article, they showed that efficient endocytic cycling is required for the maintenance of polarized localization of membrane proteins, by demonstrating that in the endocytosis-defective mutant, Snc1p loses its polarized localization. They propose that mutants defective in the assembly of cortical actin patches lose their polarized localization because they are defective in endocytosis, not because they cannot assemble cortical actin patches. Similarly, the *cdc50*Δ mutant shows depolarization of cortical actin patches possibly due to its defects in endocytic cycling. Because Cdc42p is required for polarized assembly of cortical actin patches and actin cables, defects in cell polarity in the *cdc50*Δ mutant may be accounted for by defective endocytic cycling of Cdc42p and its effectors, Bni1p and Gic1p. Intracellular stainings of Bni1p-GFP and Gic1p-GFP in the *cdc50*Δ mutant might represent their intermediates in their endocytic recycling pathway.

ACKNOWLEDGMENTS

We thank Charles Boone, Michael Lewis, Hugh Pelham, Akihiko Nakano, and Roger Tsien for yeast strains and plasmids. We thank Kazuo Emoto, Takaharu Yamamoto, and the members of the Tanaka laboratory for valuable discussion. We also thank Aiko Ishioh, Toshika Matsumoto, and Eriko Itoh for technical assistance. K.S. is especially grateful to Ayumi Saito for encouragement during this work. This work was supported by grants-in-aid for scientific research from the Ministry of Education, Culture, Sports, Science and Technology, Japan, to K.F.-K. and K.T.

REFERENCES

Agatep, R., Kirkpatrick, R.D., Parchaliuk, D.L., Woods, R.A., and Gietz, R.D. (1998). Transformation of *Saccharomyces cerevisiae* by the lithium acetate/single-stranded carrier D.N.A/polyethylene glycol (LiAc/ss-D.N.A/P.E.G) protocol. Technical Tips Online. Available at: http//research.bmn.com/tto. Search for "lithium acetate" from the opening page. Accessed May 2, 2003

Beggah, A., Mathews, P., Beguin, P., and Geering, K. (1996). Degradation and endoplasmic reticulum retention of unassembled α- and β-subunits of Na,K-ATPase correlate with interaction of BiP. J. Biol. Chem. *271*, 20895–20902.

Berkower, C., Loayza, D., and Michaelis, S. (1994). Metabolic instability and constitutive endocytosis of *STE6*, the a-factor transporter of *Saccharomyces cerevisiae*. Mol. Biol. Cell *5*, 1185–1198.

Brown, J.L., Jaquenoud, M., Gulli, M.P., Chant, J., and Peter, M. (1997). Novel Cdc42-binding proteins Gic1 and Gic2 control cell polarity in yeast. Genes Dev. *11*, 2972–2982.

Campbell, R.E., Tour, O., Palmer, A.E., Steinbach, P.A., Baird, G.S., Zacharias, D.A., and Tsien, R.Y. (2002). A monomeric red fluorescent protein. Proc. Natl. Acad. Sci. USA *99*, 7877–7882.

Catty, P., de Kerchove d'Exaerde, A., and Goffeau, A. (1997). The complete inventory of the yeast *Saccharomyces cerevisiae* P-type transport ATPases. FEBS Lett. *409*, 325–332.

Cerbon, J., and Calderon, V. (1991). Changes of the compositional asymmetry of phospholipids associated to the increment in the membrane surface potential. Biochim. Biophys. Acta *1067*, 139–144.

Chang, A., and Slayman, C.W. (1991). Maturation of the yeast plasma membrane [H+] ATPase involves phosphorylation during intracellular transport. J. Cell Biol. *115*, 289–295.

Chardin, P., Paris, S., Antonny, B., Robineau, S., Beraud-Dufour, S., Jackson, C.L., and Chabre, M. (1996). A human exchange factor for ARF contains Sec7- and pleckstrin-homology domains. Nature *384*, 481–484.

Chen, C.Y., Ingram, M.F., Rosal, P.H., and Graham, T.R. (1999). Role for Drs2p, a P-type ATPase and potential aminophospholipid translocase, in yeast late Golgi function. J. Cell Biol. *147*, 1223–1236.

Chen, G.C., Kim, Y.J., and Chan, C.S. (1997). The Cdc42 GTPase-associated proteins Gic1 and Gic2 are required for polarized cell growth in *Saccharomyces cerevisiae*. Genes Dev. *11*, 2958–2971.

Devaux, P.F. (1991). Static and dynamic lipid asymmetry in cell membranes. Biochemistry *30*, 1163–1173.

Diaz, C., and Schroit, A.J. (1996). Role of translocases in the generation of phosphatidylserine asymmetry. J. Membr. Biol. *151*, 1–9.

Drubin, D.G., and Nelson, W.J. (1996). Origins of cell polarity. Cell *84*, 335–344.

Elble, R. (1992). A simple and efficient procedure for transformation of yeasts. Biotechniques *13*, 18–20.

Emoto, K., and Umeda, M. (2000). An essential role for a membrane lipid in cytokinesis: regulation of contractile ring disassembly by redistribution of phosphatidylethanolamine. J. Cell Biol. *149*, 1215–1224.

Evangelista, M., Blundell, K., Longtine, M.S., Chow, C.J., Adames, N., Pringle, J.R., Peter, M., and Boone, C. (1997). Bni1p, a yeast formin linking Cdc42p and the actin cytoskeleton during polarized morphogenesis. Science *276*, 118–122.

Evangelista, M., Pruyne, D., Amberg, D.C., Boone, C., and Bretscher, A. (2002). Formins direct Arp2/3-independent actin filament assembly to polarize cell growth in yeast. Nat. Cell Biol. *4*, 32–41.

Fadok, V.A., Bratton, D.L., Rose, D.M., Pearson, A., Ezekewitz, R.A., and Henson, P.M. (2000). A receptor for phosphatidylserine-specific clearance of apoptotic cells. Nature *405*, 85–90.

Farge, E., and Devaux, P.F. (1992). Shape changes of giant liposomes induced by an asymmetric transmembrane distribution of phospholipids. Biophys. J. *61*, 347–357.

Farge, E., Ojcius, D.M., Subtil, A., and Dautry-Varsat, A. (1999). Enhancement of endocytosis due to aminophospholipid transport across the plasma membrane of living cells. Am. J. Physiol. *276*, C725–C733.

Franzusoff, A., Redding, K., Crosby, J., Fuller, R.S., and Schekman, R. (1991). Localization of components involved in protein transport and processing through the yeast Golgi apparatus. J. Cell Biol. *112*, 27–37.

Geering, K. (1990). Subunit assembly and functional maturation of Na,K-ATPase. J. Membr. Biol. *115*, 109–121.

Geering, K., Beggah, A., Good, P., Girardet, S., Roy, S., Schaer, D., and Jaunin, P. (1996). Oligomerization and maturation of Na,K-ATPase: functional interaction of the cytoplasmic NH_2 terminus of the β subunit with the α subunit. J. Cell Biol. *133*, 1193–1204.

Geli, M.I., and Riezman, H. (1998). Endocytic internalization in yeast and animal cells: similar and different. J. Cell Sci. *111*, 1031–1037.

Gerst, J.E. (1997). Conserved α-helical segments on yeast homologs of the synaptobrevin/VAMP family of v-SNAREs mediate exocytic function. J. Biol. Chem. *272*, 16591–16598.

Gietz, R.D., and Sugino, A. (1988). New yeast-*Escherichia coli* shuttle vectors constructed with *in vitro* mutagenized yeast genes lacking six-base pair restriction sites. Gene *74*, 527–534.

Goldstein, A.L., and McCusker, J.H. (1999). Three new dominant drug resistance cassettes for gene disruption in *Saccharomyces cerevisiae*. Yeast *15*, 1541–1553.

Gomes, E., Jakobsen, M.K., Axelsen, K.B., Geisler, M., and Palmgren, M.G. (2000). Chilling tolerance in *Arabidopsis* involves ALA1, a member of a new family of putative aminophospholipid translocases. Plant Cell *12*, 2441–2454.

Govindan, B., Bowser, R., and Novick, P. (1995). The role of Myo2, a yeast class V myosin, in vesicular transport. J. Cell Biol. *128*, 1055–1068.

Guthrie, C., and Fink, G.R., eds. (1991). Guide to Yeast Genetics and Molecular Biology. San Diego, CA: Academic Press.

Hanson, P.K., Malone, L., Birchmore, J.L., and Nichols, J.W. (2003). Lem3p is essential for the uptake and potency of alkylphosphocholine drugs, edelfosine and miltefosine. J. Biol. Chem. *278*, 36041–36050.

Hua, Z., Fatheddin, P., and Graham, T.R. (2002). An essential subfamily of Drs2p-related P-type ATPases is required for protein trafficking between Golgi complex and endosomal/vacuolar system. Mol. Biol. Cell *13*, 3162–3177.

Hua, Z., and Graham, T.R. (2003). Requirement for Neo1p in retrograde transport from the Golgi complex to the endoplasmic reticulum. Mol. Biol. Cell *14*, 4971–4983.

Jaquenoud, M., and Peter, M. (2000). Gic2p may link activated Cdc42p to components involved in actin polarization, including Bni1p and Bud6p (Aip3p). Mol. Biol. Cell *20*, 6244–6258.

Jin, H., and Amberg, D.C. (2000). The secretory pathway mediates localization of the cell polarity regulator Aip3p/Bud6p. Mol. Biol. Cell *11*, 647–661.

Kato, U., Emoto, K., Fredriksson, C., Nakamura, H., Ohta, A., Kobayashi, T., Murakami-Murofushi, K., and Umeda, M. (2002). A novel membrane protein, Ros3p, is required for phospholipid translocation across the plasma membrane in *Saccharomyces cerevisiae.* J. Biol. Chem. *277*, 37855–37862.

Kawasaki, R., Fujimura-Kamada, K., Toi, H., Kato, H., and Tanaka, K. (2003). The upstream regulator, Rsr1p, and downstream effectors, Gic1p and Gic2p, of the Cdc42p small GTPase coordinately regulate initiation of budding in *Saccharomyces cerevisiae.* Genes Cells *8*, 235–250.

Lewis, M.J., Nichols, B.J., Prescianotto-Baschong, C., Riezman, H., and Pelham, H.R. (2000). Specific retrieval of the exocytic SNARE Snc1p from early yeast endosomes. Mol. Biol. Cell *11*, 23–38.

Longtine, M.S., McKenzie, A., Demarini, D.J., Shah, N.G., Wach, A., Brachat, A., Philippsen, P., and Pringle, J.R. (1998). Additional modules for versatile and economical PCR-based gene deletion and modification in *Saccharomyces cerevisiae.* Yeast *14*, 953–961.

Marx, U., Polakowski, T., Pomorski, T., Lang, C., Nelson, H., Nelson, N., and Herrmann, A. (1999). Rapid transbilayer movement of fluorescent phospholipid analogues in the plasma membrane of endocytosis-deficient yeast cells does not require the Drs2 protein. Eur. J. Biochem. *263*, 254–263.

Misu, K., Fujimura-Kamada, K., Ueda, T., Nakano, A., Katoh, H., and Tanaka, K. (2003). Cdc50p, a conserved endosomal membrane protein, controls polarized growth in *Saccharomyces cerevisiae.* Mol. Biol. Cell *14*, 730–747.

Mochida, J., Yamamoto, T., Fujimura-Kamada, K., and Tanaka, K. (2002). The novel adaptor protein, Mti1p, and Vrp1p, a homolog of Wiskott-Aldrich syndrome protein-interacting protein (WIP), may antagonistically regulate type I myosins in *Saccharomyces cerevisiae.* Genetics *160*, 923–934.

Moir, D., Stewart, S.E., Osmond, B.C., and Botstein, D. (1982). Cold-sensitive cell-division-cycle mutants of yeast: isolation, properties, and pseudoreversion studies. Genetics *100*, 547–563.

Munn, A.L., Stevenson, B.J., Geli, M.I., and Riezman, H. (1995). *end5*, end6, and *end7*, mutations that cause actin delocalization and block the internalization step of endocytosis in Saccharomyces cerevisiae. Mol. Biol. Cell *6*, 1721–1742.

Piper, R.C., Cooper, A.A., Yang, H., and Stevens, T.H. (1995). *VPS27* controls vacuolar and endocytic traffic through a prevacuolar compartment in *Saccharomyces cerevisiae.* J. Cell Biol. *131*, 603–617.

Pomorski, T., Lombardi, R., Riezman, H., Devaux, P.F., Van Meer, G., and Holthuis, J.C. (2003). Drs2p-related P-type ATPases Dnf1p and Dnf2p are required for phospholipid translocation across the yeast plasma membrane and serve a role in endocytosis. Mol. Biol. Cell *14*, 1240–1254.

Prezant, T.R., Chaltraw, W.E., Jr., and Fischel-Ghodsian, N. (1996). Identification of an overexpressed yeast gene which prevents aminoglycoside toxicity. Microbiology *142*, 3407–3414.

Pringle, J.R., Bi, E., Harkins, H.A., Zahner, J.E., De Virgilio, C., Chant, J., Corrado, K., and Fares, H. (1995). Establishment of cell polarity in yeast. Cold Spring Harb. Symp. Quant. Biol. *60*, 729–744.

Pruyne, D., and Bretscher, A. (2000). Polarization of cell growth in yeast. J. Cell Sci. *113*, 571–585.

Radji, M., Kim, J.M., Togan, T., Yoshikawa, H., and Shirahige, K. (2001). The cloning and characterization of the *CDC50* gene family in *Saccharomyces cerevisiae.* Yeast *18*, 195–205.

Rose, M.D., Winston, F., and Hieter, P. (1990). Methods in Yeast Genetics: A Laboratory Course Manual. Cold Spring Harbor, NY: Cold Spring Harbor Laboratory Press.

Rosing, J., Tans, G., Govers-Riemslag, J.W., Zwaal, R.F., and Hemker, H.C. (1980). The role of phospholipids and factor Va in the prothrombinase complex. J. Biol. Chem. *255*, 274–283.

Rothman, J.E., and Lenard, J. (1977). Membrane asymmetry. Science *195*, 743–753.

Sagot, I., Klee, S.K., and Pellman, D. (2002). Yeast formins regulate cell polarity by controlling the assembly of actin cables. Nat. Cell Biol. *4*, 42–50.

Sato, M., Sato, K., and Nakano, A. (2004). ER quality control of unassembled iron transporter depends on Rer1p-mediated retrieval from the Golgi. Mol. Biol. Cell *15*, 1417–1424.

Schott, D., Ho, J., Pruyne, D., and Bretscher, A. (1999). The COOH-terminal domain of Myo2p, a yeast myosin V, has a direct role in secretory vesicle targeting. J. Cell Biol. *147*, 791–807.

Siegmund, A., Grant, A., Angeletti, C., Malone, L., Nichols, J.W., and Rudolph, H.K. (1998). Loss of Drs2p does not abolish transfer of fluorescence-labeled phospholipids across the plasma membrane of *Saccharomyces cerevisiae.* J. Biol. Chem. *273*, 34399–34405.

Takei, K., Haucke, V., Slepnev, V., Farsad, K., Salazar, M., Chen, H., and De Camilli, P. (1998). Generation of coated intermediates of clathrin-mediated endocytosis on protein-free liposomes. Cell *94*, 131–141.

Tang, N., Lin, T., and Ostap, E.M. (2002). Dynamics of Myo1c (Myosin-Iβ) lipid binding and dissociation. J. Biol. Chem. *277*, 42763–42768.

Tang, X., Halleck, M.S., Schlegel, R.A., and Williamson, P. (1996). A subfamily of P-type ATPases with aminophospholipid transporting activity. Science *272*, 1495–1497.

Valdez-Taubas, J., and Pelham, H.R. (2003). Slow diffusion of proteins in the yeast plasma membrane allows polarity to be maintained by endocytic cycling. Curr. Biol. *13*, 1636–1640.

Vida, T.A., and Emr, S.D. (1995). A new vital stain for visualizing vacuolar membrane dynamics and endocytosis in yeast, J. Cell Biol. *128*, 779–792.

Wedlich-Soldner, R., Altschuler, S., Wu, L., and Li, R. (2003). Spontaneous cell polarization through actomyosin-based delivery of the Cdc42 GTPase. Science *299*, 1231–1235.

Wendland, B., Emr, S.D., and Riezman, H. (1998). Protein traffic in the yeast endocytic and vacuolar protein sorting pathways. Curr. Opin. Cell Biol. *10*, 513–522.